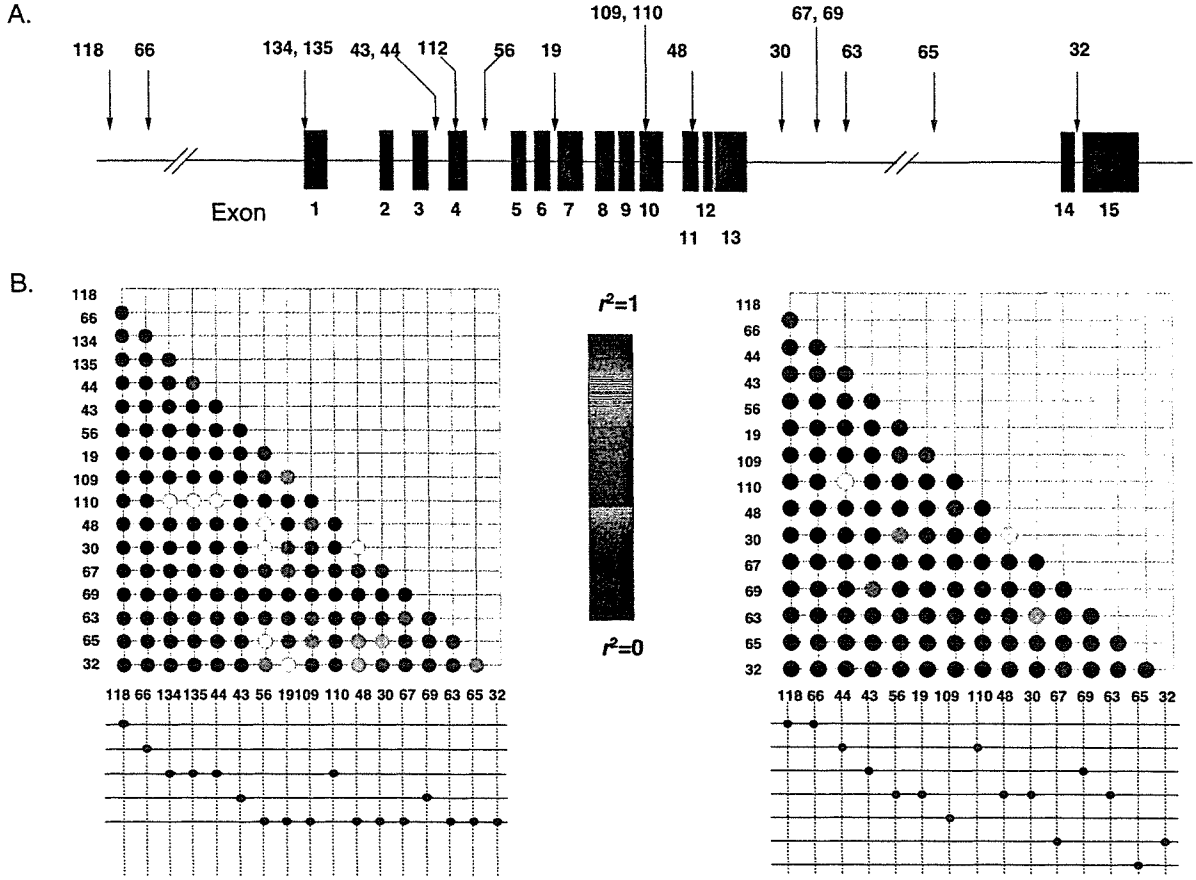

Fig. 2. A. Exon-intron organization of *CAPN10*. The physical distance between SNP-118 and SNP-32 is approximately 40 kb. The locations of the SNPs are shown.
B. Pairwise linkage disequilibrium in *CAPN10* evaluated by r^2. All SNP numbers are denoted in Fig. 2A. Pairwise LD was determined using 136 and 105 marker pairs in Japanese (left panel) and Mexican Americans (right panel), respectively. SNP-134 and -135 were not identified in the previous study with Mexican Americans [5]. The color gradations from red (perfect LD, *i.e.*, $r^2 = 1$) to blue (no LD, *i.e.*, $r^2 = 0$) reflect the degree of the observed LD. Subgroups of SNPs found in tight linkage (r^2>0.5) also are shown. Since there was no suitable polymorphic site upstream of *CAPN10* [5], we used SNP-118 and -66 in the study, despite their low allele frequencies.

selection model but requires a multiallele selection model with sequential turnover of polymorphisms. Thus, a complicated population structure other than natural selection may be involved in this feature, but that alone cannot explain the rapid decline in LD. For loci such as intron 13 of calpain-10 that exhibit a rapid decline in LD, a high recombination rate is generally reported. Although no studies have reported a correlation between the recombination rate and the frequency of polymorphisms, exceptional recombination or mutation in a neutral state is possible [23]. Recently, a close analysis of intron 13 showed that a selection model consisting of five clusters of haplotypes can explain the genetic findings in Mexican Americans, two of the five clusters appearing 2 to 3 million years ago

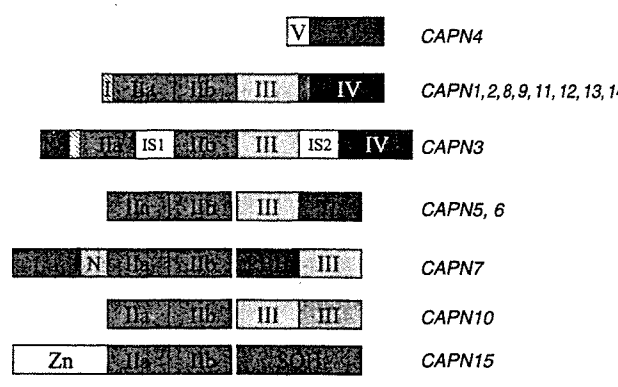

Fig. 3. Domain structures of the human calpain family
Typical calpains are composed of four domains (I–IV), but in the case of atypical calpains, certain domains have been deleted or replaced. The small subunit of calpain is composed of two domains.

in the glacial ages. Comparisons of the partial sequence at intron 13 among 10 species show that four USF1 and one HNF1 binding sites in a segment share common sequence motifs. In addition, an unknown gene is expressed around the segment that might influence calpain-10 expression [24].

Calpains

Calpains are a family of cytoplasmic cysteine proteases activated by Ca^{2+}. At least 15 calpains have been identified as eight typical calpains, six atypical calpains, and one small subunit of calpain [25, 26]. The domain structures of the calpain family are shown in Fig. 3. Known substrates for calpains include cytoskeletal proteins, actin-binding proteins, calmodulin-binding proteins, hormone receptors, cell membrane hormone receptors, glucose-metabolizing enzymes, enzymes regulating signal transmission, and transcription factors. Calpains are known to play a physiological role in reconstruction of cytoskeleton, apoptosis, and reconstruction (proliferation, differentiation, and transformation) of tissue cells. Mutations in genes encoding calpains cause various disorders including diabetes related to calpain-10, gastric cancer related to calpain-9, muscular dystrophy related to calpain-3, neurodegenerative diseases (*e.g.*, Alzheimer's disease), cerebral infarction, spinal injury, myocardial infarction, hepatic ischemia, and renal impairment. Animal tests show death in the fetal period in calpain-4 (small subunit) knockout mice due to impaired development of the cardiovascular system. Calpain-1 knockout mice develop normally because the lost function of calpain-1 is compensated by calpain-2, but the mice often show platelet aggregation disorder.

Calpain-10

The human calpain-10 gene is located in chromosome band 2q37.3 and consists of 15 exons. There are at least eight isoforms (calpain-10a to calpain-10h) of the gene. The longest isoform, calpain-10a, consists of 672 amino acids. Calpain-10 is an atypical calpain that lacks domain IV and instead has a tandem linking domain, domain III. Calpain-10a is expressed most strongly in the heart, but is present in various tissues including those playing an important role in glucose metabolism, including liver, muscle, pancreatic islets, and adipocytes [5, 25]. Although calpain-10c and 10g can be detected in many tissues, calpain-10b, 10d, 10e, and 10f are much less abundant [5]. Because calpain-10 lacks calcium-binding sites in domains II and III, it is not known whether the protein is activated by calcium. Calpain-10 may react with calcium in a separate mechanism, as it can be found in sarcomere, the calcium storage in muscle fibre, and its expression is increased or its distribution is altered following calcium stimulation in the epithelium of crystalline [27].

Effects of calpain-10

Effects of calpain-10 on β cells

1) Calpain and apoptosis

Involvement of calpain-10 in ryanodine-induced apoptosis was reported based on finding that apoptosis was enhanced by ryanodine or palmitin acid in pancreatic β cell-specific calpain-10 transgenic mice by the rat insulin promoter but was not enhanced in calpain-10 knockout mice [28].

2) Calpain and insulin secretion

The relationship between calpain and insulin secretion was assessed with calpain inhibitors. Assessed with a nonspecific calpain inhibitor, glucose-responsive insulin secretion was enhanced in short-term culture with the inhibitor added, while insulin secretion was inhibited by reduced mitochondrial glucose metabolism in 48-hour culture with the inhibitor added [29, 30].

Calpain-1, a typical calpain, is reported to break ICA512, a tyrosine phosphatase-like protein located in insulin granules, dependent on the intracellular Ca^{2+} concentrations. A calpain inhibitor blocked the breakage, thereby impairing insulin secretion [31]. In a recently reported assay system in which calpain-10 was overexpressed stably in INS1 cells, glucose-responsive insulin secretion was enhanced. The breakage was reduced by the addition of E64, a calpain inhibitor, to the cells. When Ca^{2+} was removed from the supernatant, these reactions were not induced. These results indicate that the intracellular Ca^{2+} concentration increased by glucose stimulation can activate calpain-10 and break SNAP25 (a SNARE protein), thereby inducing fusion of insulin granules to the membrane of the β cells [32]. However, considering the

absence of key 54-kD proteins among the reported calpain-10 isoforms, further analysis is required.

Effects of calpain-10 on muscles

In clinical research assessing the relationship between SNP-43G/G and the level of calpain-10 mRNA expression in Pima Indians, individuals with the SNP-43G/G allele were found to have a low level of expression. A significant association was also found between oxidative utilization of glucose and the level of calpain-10 expression [33]. In an animal study using mice expressing calpastatin (a calpain inhibitor) in muscles, muscular glucose uptake and general glucose tolerance remained unchanged despite increased expression of GLUT4 protein and muscular hypertrophy mainly due to loss of insulin action resulting from reduced AKT kinase activity [34]. However, while calpastatin inhibits the activity of calpain-1 and calpain-2, action on calplain-10 is unlikely since calpain 10 does not bind with the calpain small subunit (calpain-4), the target of calpastatin. In an *in-vitro* study with human myoblasts to assess the relationship between calpain-10 and muscle differentiation, 60 kD calpain-10 protein levels were found to increase as differentiation progressed [35]. As differentiation of the myoblasts progressed, calpain-1 levels also increased and calpastatin expression decreased. In L8 cells over-expressing calpastatin, muscle differentiation was inhibited [36–38]. These findings demonstrate the involvement of calpain-10 as well as the calpain-calpastatin system in the process of myoblast differentiation.

Effects of calpain-10 on adipocytes

Some groups have investigated the function of adipocytes in association with calpains, but no relationship between SNP43 and obesity was noted. In an *in-vitro* study using human adipocytes, adipogenesis in adipocytes was increased in a group with the SNP-43G/G allele irrespective of the level of GLUT4 expression. Lipolysis function from β3 adrenalin receptors was reduced in a group with the SNP19-deficient allele to one-thirtieth that in the normal group [39, 40]. In a clinical study, the level of calpain-10 mRNA expression in adipocytes decreased dependent on the blood triglyceride level in obese patients with the SNP43G/G allele [41]. In calpain-10 antisense-expressing stable cell line 3T3L1 adipocytes, actin reconstruction was inhibited by insulin with an unchanged level of GLUT4 expression, resulting in reduced glucose uptake and inhibited transfer of GLUT4 to the membrane by insulin [42]. As in other reports on the relationship between calpains and adipocytes, the level of calpain-1 expression increased while calpastatin expression decreased as adipocyte differentiation progressed, and when the action of calpain was inhibited by forced expression of calpastatin or the addition of the calpain inhibitor, C/EBPα expression and adipocyte differentiation were inhibited [43].

Clinical assessment of calpain-10

An analysis in nondiabetic British subjects revealed that genetic variation in the *CAPN10* gene influences blood glucose levels and that this is, at least in part, due to the effects of calpain-10 on early insulin secretory response [44]. An analysis in Finns showed that individuals with the1121/1121-haplotype combination for SNP-44, -43, -19, or -63 have approximately two times higher risk of development of diabetes, and that SNP-43 is associated with high fasting insulin levels, high HOMA-R levels, and high fasting fatty acid levels [45]. An analysis in Japanese found no significant association between diabetes and these haplotype combinations, but did find an association with insulin resistance and high fatty acid levels under euglycemic hyperinsulinemic clamp in individuals with the 112/121 haplogenotype [17] (Table 1).

Relationship between calpain-10 and diabetes-related diseases

For polycystic ovary syndrome, no phenotypic differences were noted among non-diabetic European Americans with a single polymorphism or haplotype of SNP-43, -19, or -63. In non-diabetic African American probands, no single polymorphism of SNP-43, -19, or -63 was associated with any phenotype, but individuals with the 112/121-haplotype combination showed a significantly greater area under the insulin-time curve on oral glucose tolerance test. This result was evident after data adjustment for body mass index. In African Americans and European Americans, the 112/121-haplotype combination was associated with approximately two times higher risk of polycystic ova-

Table 1. Association studies of *CAPN10* in various populations

Population	Genotype	Odds Ratio	Phenotype
Mexican American	112/121	3.02 (1.37–6.64)	
Pima Indian	SNP-43 G/G		Glucose utilization ↓
	111/111	2.04 (1.22–3.39)	
British/Irish Whites	2111/2111	2.52 (1.06–5.97)	
	2111/1111	2.36 (1.19–4.66)	A.I.R ↓
	112/121		HOMA-R ↑
Samoans	112/121	1.42 (0.68–2.98)	
Utah-Caucasian	111/221	1.48 (1.06–1.91)	Insulin AUC ↑
	SNP-19-63		HOMA-R ↑
African-American	SNP-43 G/G	1.38 (1.04–1.83)	Insulin AUC ↑
	112/121	2.18 (1.06–4.45)	PCOS Odds Ratio ↑
Spanish	SNP-44 CC, TC	2.57 (1.22–5.44)	PCOS Odds Ratio ↑
Polish	121/121	1.93 (1.03–3.54)	
Finnish	1121/1121	1.93 (1.07–3.47)	Fasting Insulin HOMA-RFFA ↑
Japanese	112/121		FFA ↑
	121/121		Protective against T2DM ↑

The results of studies with various populations are shown in this slide. The major (1) and minor (2) alleles are denoted as in Mexican Americans.
A.I.R, Acute Insulin Response; A.U.C, Area Under Curve; HOMA-R, Homeostasis Model Assessment-Resistance; FFA, Free Fatty Acid

ry syndrome [46]. In Spanish, an association between UCSNP44 and the incidence of polycystic ovary syndrome was reported [47].

Protease inhibitors and diabetes

Protease inhibitors are effective in the treatment of HIV infection. However, long-term use appears to induce pathology of hyperlipidemia or diabetes, including peripheral fatty atrophy and central fatty hypertrophy [48]. The mechanism is thought to be inhibited adipocyte differentiation. Calpain inhibitors, a type of protease inhibitor, are considered in the treatment of several disorders including spinal injury, liver transplantation, and myocardial infarction. Since calpain inhibitors inhibit adipocyte differentiation, attention must be paid to the possibility of diabetes and hyperlipidemia when they are used.

Conclusions

Ethnic comparison of polymorphisms can clarify the association of genetic structure with disease and play an important role in supporting case-control results. The approach is especially useful in screening putative susceptibility genes for common diseases that may have undergone recent natural selection, including those for type 2 diabetes. Sequence determination of a naturally selected segment can both identify a susceptibility gene and the mechanism of its regulation. Because of the recent, remarkable progress in sequencing techniques, identification of all of the polymorphisms on the entire human genome, SNPs in particular, may soon be possible. However, the enormous cost of SNP typing remains a limiting factor for their use in investigations of ethnic variants in common diseases. Association studies based on haplotype analysis can identify susceptibility genes, calculate developmental risks, and predict drug responsiveness. Translational research on function using interactome, proteome, and model mice can be used to apply the results clinically as individualized therapy.

Acknowledgement

We thank S. Oike, R. Kawakami, Y. Yaginuma, I. Uda, J. Tsutsumi, Y. Ibe, and T. Takahashi for assistance. The study was supported by Grant-in-Aid for Scientific Research and for Scientific Research on Priority Areas (C) "Medical Genome Science" from the Japanese Ministry of Science, Education, Sports,

Culture and Technology; a Health and Labor Science Research Grant for Research on Human Genome and Tissue Engineering from the Japanese Ministry of Health, Labor and Welfare; and the Naito Foundation.

References

1. Garner C, Slatkin M (2003) On selecting markers for association studies: Patterns of linkage disequilibrium between two and three diallelic loci. *Genet Epidemiol* 24: 57–67.
2. Ioannidis JPA, Trikalinos TA, Ntzani EE, Contopoulos-Ioannidis DG (2003) Genetic associations in large versus small studies: an empirical assessment. *Lancet* 361: 567–571.
3. Hanis CL, Boerwinkle E, Chakraborty R, Ellsworth DL, Concannon P, Stirling B, Morrison VA, Wapelhorst B, Spielman RS, Gogolin-Ewens KJ, Shephard JM, Williams SR, Risch N, Hinds D, Iwasaki N, Ogata M, Omori Y, Petzold C, Rietzsch H, Schroder HE, Schulze J, Cox NJ, Menzel S, Boriraj VV, Chen X, Lim LR, Lindner T, Mereu LE, Wang YQ, Xiang K, Yamagata K, Yang Y, Bell GI (1996) A genome-wide search for human non-insulin-dependent (type 2) diabetes genes reveals a major susceptibility locus on chromosome 2. *Nat Genet* 13: 161–166.
4. Excoffer L, Slatkin M (1995) Maximum-likelihood estimation of molecular haplotype frequencies in a diploid population. *Mol Biol Evol* 12: 921–927.
5. Horikawa Y, Oda N, Cox NJ, Li X, Orho-Melander M, Hara M, Hinokio Y, Lindner TH, Mashima H, Schwarz PEH, del Bosque-Plata L, Horikawa Y, Oda Y, Yoshiuchi I, Colilla S, Polonsky KS, Wei S, Concannon P, Iwasaki N, Schulze J, Baier LJ, Bogardus C, Groop L, Boerwinkle E, Hanis CL, Bell GI (2000) Genetic variation in the gene encoding calpain-10 is associated with type 2 diabetes mellitus. *Nat Genet* 26: 163–175.
6. Evans JC, Frayling TM, Cassell PG, Saker PJ, Hitman GA, Walker M, Levy JC, O'Rahilly S, SubbaRao PV, Bennett AJ, Jones EC, Menzel S, Prestwich P, Simecek N, Wishart M, Dhillon R, Fletcher C, Millward A, Demaine A, Wilkin T, Horikawa Y, Cox NJ, Bell GI, Ellard S, McCarthy MI, Hattersley AT (2001) Association studies of the calpain-10 gene with type 2 diabetes mellitus in the United Kingdom. *Am J Hum Genet* 69: 544–552.
7. Weedon MN, Schwarz PEH, Horikawa Y, Iwasaki N, Illig T, Holle R, Rathmann W, Selisko T, Schulze J, Owen KR, Evans J, del Bosque-Plata L, Hitman G, Walker M, Levy JC, Sampson M, Bell GI, McCarthy MI, Hattersley AT, Frayling TM (2003) Meta-analysis confirms a role for calpain-10 variation in type 2 diabetes susceptibility. *Am J Hum Genet* 73: 1208–1212.
8. Song Y, Niu T, Manson JE, Kwiatkowski DJ, Liu S (2004) Are variants in the calpain-10 gene related to risk of type 2 diabetes? A quantitative assessment of population and family-based association studies. *Am J Hum Genet* 74: 208–222.
9. Cassell PG, Jackson AE, North BV, Evans JC, Syndercombe-Court D, Phillips C, Ramachandran A, Snehalatha C, Gelding SV, Vijayaravaghan S, Curtis D, Hitman GA (2002) Haplotype combinations of calpain-10 gene polymorphisms associate with increased risk of impaired glucose tolerance and type 2 diabetes in south Indians. *Diabetes* 51: 1622–1628.
10. Garant MJ, Linda Kao WH, Brancati F, Coresh J, Rami TM, Hanis CL, Boerwinkle E, Shuldiner AR (2002) SNP43 of *CAPN10* and the risk of type 2 diabetes in African-Americans. *Diabetes* 51: 231–237.
11. Malecki MT, Moczulski DK, Klupa T, Wanic K, Cyganek K, Frey J, Sieradzki J (2002) Homozygous combination of calpain-10 gene haplotypes is associated with type 2 diabetes mellitus in a Polish population. *Eur J Endocrinol* 146: 695–699.
12. Tsai HJ, Sun G, Weeks DE, Kaushal R, Wolujewicz M, McGarvey ST, Tufa J, Viali S, Deka R (2001) Type 2 diabetes and three calpain-10 gene polymorphisms in Samoans: No evidence of association. *Am J Hum Genet* 69: 1236–1244.
13. Fingerlin TE, Erdos MR, Watanabe RM, Wiles KR, Stringham HM, Mohlke KL, Silander K, Valle TT, Buchanan TA, Tuomilehto J, Bergman RN, Boehnke M, Collins FS (2002) Variation in three single nucleotide polymorphisms in the calpain-10 gene not associated with type 2 diabetes in a large Finnish cohort. *Diabetes* 51: 1644–1648.
14. Hegele RA, Harris SB, Zinman B, Hanley AJ, Cao H (2001) Absence of association of type 2 diabetes with *CAPN10* and *PC1* polymorphisms in Oji-Cree. *Diabetes Care* 24: 1498–1499.
15. Elbein SC, Chu W, Ren Q, Hemphill C, Schay J, Cox NJ, Hanis CL, Hasstedt SJ (2002) Role of calpain-10 gene variants in familial type 2 diabetes in Caucasians. *J Clin Endcrinol Metab* 87: 650–654.
16. Rasmussen SK, Urhammer SA, Berglund L, Jensen JN, Hansen L, Echwald SM, Borch-Johnson K, Horikawa Y, Mashima H, Lithell H, Cox NJ, Hansen T, Bell GI, Pederson O (2002) Variants within the calpain-10 gene on chromosome 2q37 (*NIDDM1*) and relationships to type 2 diabetes, insulin resistance and impaired acute insulin secretion among Scandinavian Caucasians. *Diabetes* 51: 3561–3567.

17. Horikawa Y, Oda N, Yu L, Imamura S, Fujiwara K, Makino M, Seino Y, Itoh M, Takeda J (2003) Genetic variations in *CAPN10* are not a major factor in the occurrence of type 2 diabetes in Japanese. *J Clin Endocrinol Metab* 88: 244–247.
18. Iwasaki N, Horikawa Y, Tsuchiya T, Kitamura Y, Nakamura T, Tanizawa Y, Oka Y, Hara K, Kadowaki T, Awata T, Honda M, Yamashita K, Oda N, Yu L, Yamada N, Ogata M, Kamatani N, Iwamoto Y, Hanis CL, del Bosque-Plata L, Hayes MG, Cox NJ, Bell GI (2005) Genetic variants in the calpain-10 gene and the development of type 2 diabetes in the Japanese population. *J Hum Genet* 50: 92–98.
19. Fullerton SM, Bartoszewics A, Ybazeta G, Horikawa Y, Bell GI, Kidd KK, Cox NJ, Hudson RR, DiRienzo A (2002) Geographic and haplotype structure of candidate type 2 diabetes susceptibility variants at the calpain-10 locus. *Am J Hum Genet* 70: 1096–1106.
20. Altshuler D, Hirschhorn JN, Klannemark M, Lindgren CM, Vohl MC, Nemesh J, Lane CR, Schaffner SF, Bolk S, Brewer C, Tuomi T, Gaudet D, Hudson TJ, Daly M, Groop L, Lander ES (2000) The common PPARgamma Pro12Ala polymorphism is associated with decreased risk of type 2 diabetes. *Nat Genet* 26: 76–80.
21. Stengard JH, Zerba KE, Pekkanen J, Ehnholm C, Nissinen A, Sing CF (1995) Apolipoprotein E polymorphism predicts death from coronary heart disease in a longitudinal study of elderly Finnish men. *Circulation* 91: 265–269.
22. Corder EH, Saunders AM, Strittmatter WJ, Schmechel DE, Gaskell PC, Small GW, Roses AD, Haines JL, Pericak-Vance MA (1993) Gene dose of apolipoprotein E type 4 allele and the risk of Alzheimer's disease in late onset families. *Science* 261: 921–923.
23. Vander Molen J, Frisse LM, Fullerton SM, Qian Y, del Bosque-Plata L, Hudson RR, DiRienzo A (2005) Population genetics of *CAPN10* and *GPR35*: implications for the evolution of type 2 diabetes variants. *Am J Hum Genet* 76: 548–560.
24. Clark VJ, Cox NJ, Hammond M, Hanis CL, DiRienzo A (2005) Haplotype structure and phylogenetic shadowing of a hypervariable region in the *CAPN10* gene. *Hum Genet* (epub).
25. Suzuki K, Hata S, Kawabata Y, Sorimachi H (2004) Sructure, activation, and biology of calpain. *Diabetes* 53: S12–S18.
26. Goll DE, Thompson VF, Li H, Wei W, Cong J (2002) The calpain system. *Physiol Rev* 83: 731–801.
27. Ma H, Fukiage C, Kim YH, Duncan MK, Reed NA, Shih M, Azuma M, Shearer TR (2001) Characterization and expression of calpain 10. A novel ubiquitous calpain with nuclear localization. *J Biol Chem* 276: 28525–28531.
28. Johnson JD, Han Z, Otani K, Ye H, Zhang Y, Wu H, Horikawa Y, Misler S, Bell GI, Polonsky KS (2004) RyR2 and calpain-10 delineate a novel apoptosis pathway in pancreatic islets. *J Biol Chem* 279: 24794–24802.
29. Sreenan SK, Zhou YP, Otani K, Hansen PA, Currie KPM, Pan CY, Lee JP, Ostrega DM, Pugh W, Horikawa Y, Cox NJ, Hanis CL, Burant CF, Fox AP, Bell GI, Polonsky KS (2001) Calpains play a role in insulin secretion and action. *Diabetes* 50: 2013–2020.
30. Zhou YP, Sreenan S, Pan CY, Currie KP, Bindokas VP, Horikawa Y, Lee JP, Ostrega D, Ahmed N, Baldwin AC, Cox NJ, Fox AP, MillerRJ, Bell GI, Polonsky KS (2003) A 48-hour exposure of pancreatic islets to calpain inhibitors impairs mitochondrial fuel metabolism and the exocytosis of insulin. *Metabolism* 52: 528–534.
31. Ort T, Voronov S, Guo J, Zawalich K, Froehner SC, Zawalich W, Solimena M (2001) Dephosphorylation of beta2-syntrophin and Ca2+/mu-calpain-mediated cleavage of ICA512 upon stimulation of insulin secretion. *EMBO J* 20: 4013–4023.
32. Marshall C, Hitman GA, Partridge CJ, Clark A, Ma H, Shearer TR, Turner MD (2004) Evidence that an isoform of calpain-10 is a regulator of exocytosis in pancreatic beta-cells. *Mol Endocrinol* 19: 213–224.
33. Baier LJ, Permana PA, Yang X, Pratley RE, Hanson RL, Shen GQ, Mott D, Knowler WC, Cox NJ, Horikawa Y, Oda N, Bell GI, Bogardus C (2000) A calpain-10 gene polymorphism is associated with reduced muscle mRNA levels and insulin resistance. *J Clin Invest* 106: R69–R73.
34. Otani K, Han DH, Ford EL, Garcia-Roves PM, Ye H, Horikawa Y, Bell GI, Holloszy JO, Polonsky KS (2004) Calpain system regulates muscle mass and glucose transporter GLUT4 turnover *J Biol Chem* 279: 20915–20920.
35. Logie LJ, Brown AE, Yeaman SJ, Walker M (2005) Calpain inhibition and insulin action in cultured human muscle cells. *Mol Genet Metab* 85: 54–60.
36. Barnoy S, Maki M, Kosower NS (2005) Overexpression of calpastatin inhibits L8 myoblast fusion. *Biochem Biophys Res Commun* 332: 697–701.
37. Barnoy S, Glaser T, Kosower NS (1997) Calpain and calpastatin in myoblast differentiation and fusion: effects of inhibitors. *Biochim Biophys Acta* 1358: 181–188.
38. Kwak KB, Chung SS, Kim OM, Kang MS, Ha DB, Chung CH (1993) Increase in the level of m-calpain correlates with the elevated cleavage of filamin during myogenic differentiation of embryonic muscle cells. *Biochim Biophys Acta* 1175: 243–249.
39. Hoffstedt J, Naslund E, Arner P (2002) Calpain-10 gene polymorphism is associated with reduced beta(3)-adrenoceptor function in human fat cells. *J Clin Endocrinol Metab* 87: 3362–3367.

40. Hoffstedt J, Ryden M, Lofgren P, Orho-Melander M, Groop L, Arner P (2002) Polymorphism in the Calpain 10 gene influences glucose metabolism in human fat cells. *Diabetologia* 45: 276–282.
41. Carlsson E, Fredriksson J, Groop L, Ridderstrale M (2004) Variation in the calpain-10 gene is associated with elevated triglyceride levels and reduced adipose tissue messenger ribonucleic acid expression in obese Swedish subjects. *J Clin Endcrinol Metab* 89: 3601–3605.
42. Paul DS, Harmon AW, Winston CP, Patel YM (2003) Calpain facilitates GLUT4 vesicle translocation during insulin-stimulated glucose uptake in adipocytes. *Biochem J* 376: 625–632
43. Patel YM, Lane D (1999) Role of calpain in adipocyte differentiation. *Proc Natl Acad Sci USA* 96: 1279–1285.
44. Lynn S, Evans JC, White C, Frayling TM, Hattersley AT, Turnbull DM, Horikawa Y, Cox NJ, Bell GI, Walker M (2002) Variation in the calpain-10 gene affects blood glucose levels in the British population. *Diabetes* 51: 247–250.
45. Orho-Melander M, Klannemark M, Svensson MK, Ridderstrale M, Lindgren CM, Groop L (2002) Variants in the calpain-10 gene predispose to insulin resistance and elevated free fatty acid levels. *Diabetes* 51: 2658–2664.
46. Ehrmann DA, Schwarz PE, Hara M, Tang X, Horikawa Y, Imperial J, Bell GI, Cox NJ (2002) Relationship of calpain-10 genotype to phenotypic features of polycystic ovary syndrome. *J Clin Endocrinol Metab* 87: 1669–1673.
47. Gonzalez A, Abril E, Roca A, Aragon MJ, Figueroa MJ, Velarde P, Ruiz R, Fayez O, Galan JJ, Herreros JA, Real LM, Ruiz A (2003) Specific CAPN10 gene haplotypes influence the clinical profile of polycystic ovary patients. *J Clin Endocrinol Metab* 88: 5529–5536.
48. Carr A, Samaras K, Chisholm DJ, Cooper DA (1998) Pathogenesis of HIV-1-protease inhibitor-associated peripheral lipodystrophy, hyperlipidaemia, and insulin resistance. *Lancet* 352: 1881–1883.

nature Vol 441|4 May 2006|doi:10.1038/nature04663

ARTICLES

Shugoshin collaborates with protein phosphatase 2A to protect cohesin

Tomoya S. Kitajima[1], Takeshi Sakuno[1,3], Kei-ichiro Ishiguro[1], Shun-ichiro Iemura[4], Tohru Natsume[4], Shigehiro A. Kawashima[1,2] & Yoshinori Watanabe[1,2,3]

Sister chromatid cohesion, mediated by a complex called cohesin, is crucial—particularly at centromeres—for proper chromosome segregation in mitosis and meiosis. In animal mitotic cells, phosphorylation of cohesin promotes its dissociation from chromosomes, but centromeric cohesin is protected by shugoshin until kinetochores are properly captured by the spindle microtubules. However, the mechanism of shugoshin-dependent protection of cohesin is unknown. Here we find a specific subtype of serine/threonine protein phosphatase 2A (PP2A) associating with human shugoshin. PP2A colocalizes with shugoshin at centromeres and is required for centromeric protection. Purified shugoshin complex has an ability to reverse the phosphorylation of cohesin *in vitro*, suggesting that dephosphorylation of cohesin is the mechanism of protection at centromeres. Meiotic shugoshin of fission yeast also associates with PP2A, with both proteins collaboratively protecting Rec8-containing cohesin at centromeres. Thus, we have revealed a conserved mechanism of centromeric protection of eukaryotic chromosomes in mitosis and meiosis.

Sister chromatid cohesion is carried out by a multisubunit complex, cohesin, consisting of two SMC (structural maintenance of chromosome) family proteins—a kleisin subunit Scc1/Rad21 and an accessory subunit Scc3 (also called stromal antigen (SA) in animal cells)[1–3]. Cohesion is maintained until metaphase when sister kinetochores attach to microtubules emanating from the opposite spindle poles. The cohesion at centromeres is especially important at this stage, because the establishment of bipolar spindle attachment depends on the tension generated by the pulling force of spindle microtubules and the counteracting force of centromeric cohesion of sister chromatids[4]. Indeed, in animal mitotic cells centromeric cohesin (and cohesion) persists until metaphase, whereas most cohesin dissociates from chromosome arms during prophase and prometaphase to resolve sister chromatids[3]. At the onset of anaphase, the anaphase promoting complex (APC)-dependent degradation of securin allows the activation of a specific endopeptidase, separase, which in turn cleaves and cleans off residual chromosomal Scc1/Rad21, allowing the separation of sister chromatids[5]. Thus, the dissociation of cohesin is regulated by at least two mechanisms in animal cells. During meiosis, the temporally staggered release of arm and centromeric cohesion is most striking. At the first meiotic division (meiosis I), Rec8—which replaces Scc1/Rad21 in meiosis—is cleaved along chromosome arms but is protected at centromeres, where it is only cleaved during the second division (meiosis II)[6,7].

In yeast and probably most eukaryotes, shugoshin (Sgo/MEI-S332) protects meiotic Rec8-containing cohesin from separase cleavage at meiosis I[6–12]. Human shugoshin (hSgo1; also called shugoshin-like 1 (SGOL1)), which is also expressed during proliferation, protects cohesin at centromeres for mitosis[13–15]. Phosphorylation of the cohesin subunit SA2 (an Scc3 homologue) by Polo-like kinase 1 (Plk1) is critical for prophase dissociation because the inactivation of Plk1, or the expression of a non-phosphorylatable form of SA2, substantially blocks dissociation of cohesin in early mitosis[16–18]. Moreover, the dissociation of sister chromatids in hSgo1-depleted cells is suppressed by expressing this mutant SA2 (ref. 15). In budding yeast and human cells, phosphorylation of the Scc1 subunit by Plk1 enhances its cleavability by separase[17,19,20], and this may similarly apply for the meiotic counterpart Rec8 (refs 21, 22). Therefore, a mechanism to protect cohesin at centromeres might be to inhibit its phosphorylation, but no evidence for this has been obtained as yet. It is also unknown whether shugoshin uses a similar mechanism to protect centromeric cohesin in both mitosis and meiosis. Therefore, we have investigated the mechanism by which shugoshin protects cohesin at the centromere.

Shugoshin associates with protein phosphatase 2A

To better understand shugoshin function, we sought to identify associating proteins by tagging hSgo1 with the Flag epitope and expressing the fusion protein in human embryonic kidney (HEK) 293T cells. Anti-Flag immunoprecipitates were analysed using liquid chromatography, followed by tandem mass spectrometry (LC–MS/MS)[23]. The majority of peptides identified in the analysis were those of serine/threonine protein phosphatase 2A (PP2A) (Fig. 1a). PP2A is known to act as a heterotrimeric complex consisting of a core dimer of the catalytic C subunit (PP2A-C) and the scaffold A subunit (PP2A-A), which recruits a third variable regulatory B subunit (PP2A-B/PR55/B55, PP2A-B′/PR61/B56, PP2A-B″ or PP2A-B‴) that controls substrate specificity or localization of PP2A[24]. Our MS analysis identified both core subunits PP2A-A and PP2A-C, and most isoforms of the regulatory B56 subunit, but not any isoforms of other B subunits, suggesting that hSgo1 specifically associates with PP2A containing the B56 subunit. Immunoprecipitation analysis of endogenous hSgo1 supported this conclusion (Fig. 1b) and yeast two-hybrid assays suggested direct association of hSgo1 with the PP2A-B56 subunit (Supplementary Fig. 1).

If PP2A functions together with hSgo1, PP2A would localize at the centromere during mitosis. Immunostaining experiments in HeLa cells indicated that the α isoform of PP2A-B56 (PP2A-B56α)

[1]Laboratory of Chromosome Dynamics, Institute of Molecular and Cellular Biosciences, [2]Graduate Program in Biophysics and Biochemistry, University of Tokyo, and [3]SORST, Japan Science and Technology Agency, Yayoi, Tokyo 113-0032, Japan. [4]National Institute of Advanced Industrial Science and Technology, Biological Information Research Center, Aomi, Tokyo 135-0064, Japan.

colocalizes with hSgo1 at centromeres from mitotic prophase to metaphase (Fig. 1c). The signals of both proteins decreased at the onset of anaphase. Immunostaining after chromosome spreading further indicated that PP2A-B56α localizes at the inner centromere between a pair of sister kinetochores (Fig. 1d), like hSgo1 (refs 14, 15, 25). When immunostaining for the core subunits, PP2A-A and PP2A-C, was performed in fixed cells, we found that the signals were dispersed throughout the cell (data not shown). However, by extracting mitotic cells before fixation, we could detect signals of PP2A-A and PP2A-C at centromeres in prometaphase cells but not in anaphase cells (Fig. 1e). Whereas PP2A-B56α localized only at the inner centromere, PP2A-A and PP2A-C were additionally found at spindle poles during mitosis (Fig. 1e and Supplementary Fig. 2b). These results suggest that the PP2A core complex localizes at various places within mitotic cells, including centromeres, but the PP2A complex containing the B56 subunit preferentially localizes at the inner centromere.

PP2A is required for the protection of centromeric cohesion

To directly assess the importance of PP2A for protecting sister chromatid cohesion at centromeres, we constructed short interfering (si)RNAs against *PP2A-A* and treated HeLa cells with them, which resulted in considerable reduction of PP2A-A protein (Fig. 2a). PP2A-A depletion resulted in an accumulation of mitotic cells, with the prometaphase population being particularly increased in number (Fig. 2b). Chromosomes were highly condensed and the number of spindle poles was often increased (Fig. 2c and Supplementary Fig. 2a), consistent with previous observations using okadaic acid, a potent PP2A inhibitor[26,27]. To examine centromeric cohesion, we spread the chromosomes of mitotic cells treated with *PP2A-A* siRNAs after incubation with nocodazole for 4 h. In control cells, only ~5% of mitotic cells showed separation of sister chromatids. In PP2A-A-depleted cells, however, ~15% of mitotic cells showed loosened or lost centromere cohesion, and ~30% showed sister chromatid separation (Fig. 2d, e). This separation occurred at prometaphase rather than anaphase, because most PP2A-A-depleted mitotic cells showed positive staining for cyclin B1 (Fig. 2b). Immunostaining of *PP2A-A* siRNA-treated cells with anti-Rad21 antibodies showed that cohesin localization was accordingly lost in prometaphase cells (Fig. 2f). The poor penetrance of the phenotype

a

Protein symbol	Protein name	Peptides
PPP2CA/PPP2CB	PP2A catalytic subunit C, α or β isoform	2
PPP2R1B	PP2A regulatory subunit A (PR65), β isoform	8
PPP2R5A	PP2A regulatory subunit B (B56), α isoform	7
PPP2R5B	PP2A regulatory subunit B (B56), β isoform	1
PPP2R5C	PP2A regulatory subunit B (B56), γ isoform	7
PPP2R5D	PP2A regulatory subunit B (B56), δ isoform	9
PPP2R5E	PP2A regulatory subunit B (B56), ε isoform	4
SET	SET translocation (leukaemia-associated)	5
PRO1855	Hypothetical protein PRO1855	1
RBM10/RBM5	RNA binding motif protein, 10 or 5	1
RPL10A	Ribosomal protein L10a	1
RPL28	Ribosomal protein L	1
RPL7	Ribosomal protein L7	1
RPL7A	Ribosomal protein L7a	1
RPLP1	Ribosomal protein, large, P1	1

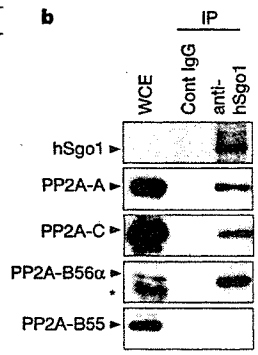

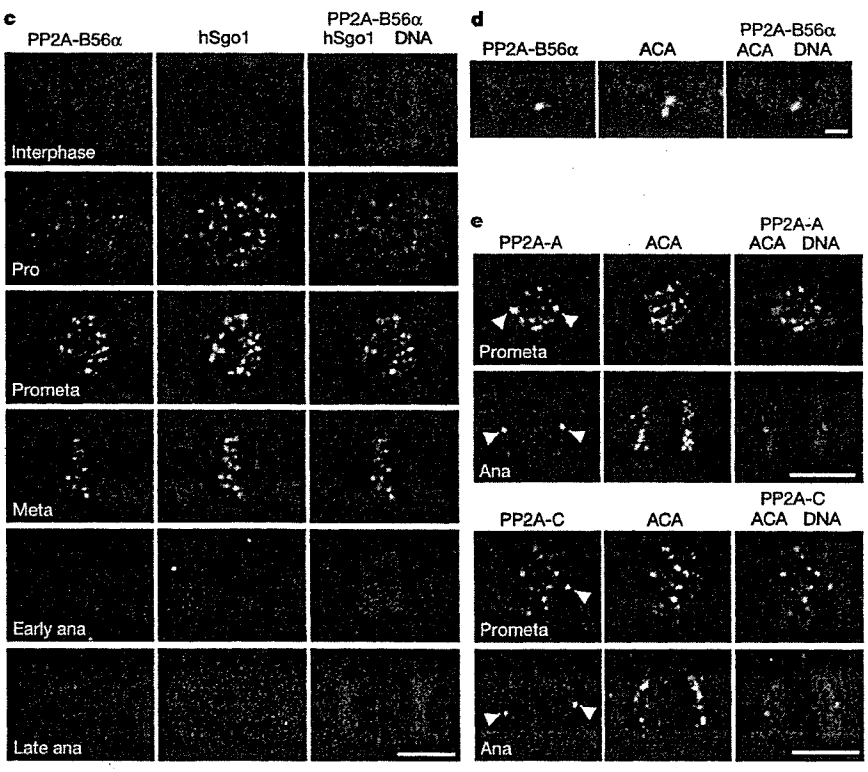

Figure 1 | PP2A associates and colocalizes with hSgo1. **a**, Proteins reproducibly detected in two independent hSgo1 immunoprecipitations by MS analysis are listed. The number of identified peptides of each protein is also shown. **b**, Immunoprecipitates (IP) from an extract of asynchronously growing HeLa cells, obtained using an anti-hSgo1 antibody or control (Cont) IgG, were analysed by western blotting using antibodies against the indicated proteins. An asterisk indicates a cross-reaction. WCE, 0.05% of the whole cell extract. **c**, HeLa cells were stained with anti-PP2A-B56α (green) and anti-hSgo1 (red) antibodies. DNA was counterstained using Hoechst 33342 (blue). PP2A-B56α colocalizes with Sgo1 at centromeres from mitotic prophase to metaphase in almost all cells ($n > 50$). Pro, prophase; Prometa, prometaphase; Meta, metaphase; Ana, anaphase. **d**, A single mitotic chromosome stained with anti-PP2A-B56α (green) and anti-centromere antibodies (ACA) (red). **e**, Mitotic cells were spun onto glass slides using a cytospin and pre-extracted before fixation. The cells were immunostained with anti-PP2A-A or anti-PP2A-C (green) and ACA (red). DNA was stained with Hoechst 33342 (blue). Signals on the spindle poles are indicated by arrowheads. Scale bars, 10 μm (**c**, **e**) and 1 μm (**d**).

after exposure to the *PP2A-A* siRNA can be explained by the residual amount of PP2A-A in the siRNA-treated cells (Fig. 2a), as a more severe phenotype was obtained by treating HeLa cells with okadaic acid (Supplementary Fig. 3). Taken together, we conclude that, like hSgo1, PP2A is required for centromeric protection of sister chromatid cohesion during prophase and prometaphase.

hSgo2 is required for the localization of PP2A at centromeres

Given that hSgo1 associates with PP2A, we examined the possibility that hSgo1 and PP2A require each other for their localization to centromeres (Fig. 3, and see also Supplementary Fig. 4). When PP2A-A was depleted by siRNA, centromeric hSgo1 signals became weakened (Fig. 3a), suggesting that PP2A has a role in facilitating hSgo1 localization to centromeres. In contrast, PP2A-B56 and PP2A-A localization was preserved at centromeres in the hSgo1-depleted cells (Fig. 3c, d), indicating that PP2A can associate with centromeres independently of hSgo1.

Human cells contain another shugoshin-like protein, hSgo2 (also known as SGOL2 and TRIPIN)[8], which has not been studied as yet. To gain a thorough understanding of the relationship between shugoshin and PP2A, we included hSgo2 in our analysis. We found that hSgo2 localizes at centromeres throughout prophase until metaphase, and disappears at anaphase (Supplementary Fig. 5), which is very similar to the localization of hSgo1 (refs 13–15, 25). Likewise, the depletion of hSgo2 using siRNA caused precocious dissociation of centromeric cohesin and separation of sister chromatids (Fig. 2), indicating that hSgo2 also functions in the centromeric protection of cohesin. The depletion of either hSgo1 or hSgo2 did not influence the localization of the other, indicating that they can independently localize to centromeres (Fig. 3a, b). Notably, the depletion of hSgo2 abolished the localization of PP2A (both the regulatory PP2A-B56 and core PP2A-A subunits) at centromeres (Fig. 3c, d). Consistent with this, PP2A coprecipitates with hSgo2; however, the association may occur through the core subunit PP2A-A

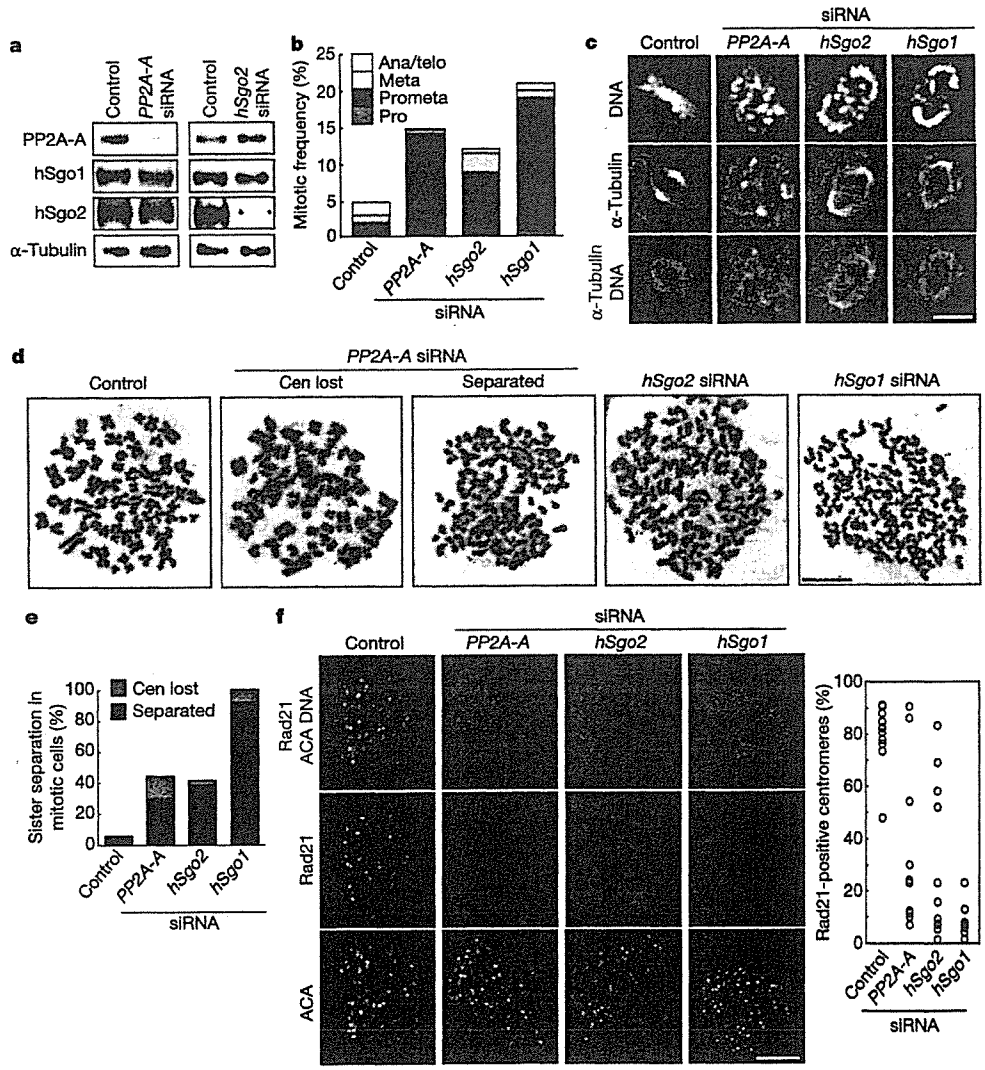

Figure 2 | PP2A is required for centromeric protection. **a**, Extracts from mitotic HeLa cells after exposure to siRNA were immunoblotted with the indicated antibodies. **b**, Mitotic index after siRNA treatment was determined by observing cell shape in living cells ($n > 560$). The mitotic phase was determined by staining for cyclin B1 and DNA in fixed cells ($n > 100$). **c**, Representative prometaphase or metaphase cells stained with anti-α-tubulin (green) and Hoechst 33342 (purple) are shown. **d**, **e**, Mitotic cells after siRNA exposure were treated with nocodazole for 4 h, and chromosomes were spread and stained with Giemsa (**d**). The frequency of cells showing sister chromatid separation ('Separated') or loss of centromeric cohesion ('Cen lost') was determined ($n > 100$) (**e**). **f**, Mitotic cells treated with the indicated siRNAs were spread by cytospin and stained with ACA (red) and anti-Rad21 (green). DNA was counterstained with Hoechst 33342 (blue). Average percentage of Rad21-positive centromeres are shown (one dot represents the average of positive centromeres within one cell). Scale bars, 10 μm (**c**, **d**, **f**).

rather than the regulatory subunit PP2A-B56 (Supplementary Figs 1 and 6). Curiously, when centromeric PP2A was displaced by *hSgo2* siRNA, hSgo1 localization was not impaired, although it was reduced by the depletion of PP2A (Fig. 3a). This may indicate that hSgo1 dynamically associates with centromeres, and that cytoplasmic PP2A may influence this interaction. If either hSgo1 or centromeric PP2A (using *hSgo2* siRNA) is absent from the centromere, the protection of sister centromeres is impaired, suggesting that both proteins collaboratively function at the centromere to protect the dissociation of cohesin.

The shugoshin complex counteracts phosphorylation of SA

Given that phosphorylation of the cohesin subunit SA2 (and presumably SA1) by Plk1 is critical for cohesin dissociation[17], we proposed that SA2 phosphorylation is counteracted by the shugoshin–PP2A complex at centromeres. To examine whether cohesin SA2 preserved around centromeres is indeed dephosphorylated *in vivo*, we prepared nocodazole-treated prometaphase cells in which cohesin is largely dissociated from the chromosome arms but tethered exclusively at centromeres, depending on shugoshin and PP2A (Fig. 2f). The cell extracts were fractionated into chromatin-bound and -unbound fractions, separated by SDS–polyacrylamide gel electrophoresis (SDS–PAGE), and blotted with anti-SA2 antibodies. As expected, SA2 showed slow electrophoretic migration in the prometaphase chromatin-unbound fraction, representing phosphorylation (presumably by Plk1)[17]. In contrast, chromatin-bound SA2 was mostly dephosphorylated (Fig. 4a). These results suggest that SA2 preserved at centromeres is dephosphorylated *in vivo*.

We next examined the biochemical properties of the shugoshin complex *in vitro*. We prepared a carboxy-terminal peptide of SA2 (SA2-C), in which most of the phosphorylation sites are included[17], and phosphorylated it with recombinant Plk1 *in vitro*. The phospho-labelled SA2 fragment was then mixed with purified hSgo1 complex. The results show that immunoprecipitates of hSgo1 can dephosphorylate SA2-C, and that this phosphatase activity is inhibitable by okadaic acid (Fig. 4b). Similar phosphatase activity was detected in the hSgo2 immunoprecipitates. These phosphatase activities also dephosphorylated a C-terminal peptide of SA1 that had been phosphorylated by Plk1, but not histone H3 phosphorylated by Aurora B kinase, indicative of substrate specificity. Thus, the shugoshin complex has the ability to counteract the phosphorylation of Scc3/SA *in vitro*. Taken together, these results support the hypothesis that PP2A-dependent dephosphorylation of Scc3/SA prevents the dissociation of cohesin from centromeres, as part of the centromeric protection function of the shugoshin complex.

PP2A is required for centromeric protection in meiosis

Schizosaccharomyces pombe Sgo1 protects centromeric cohesin containing Rec8 from separase cleavage at meiosis I[8,9]. In a yeast two-hybrid screen searching for proteins that interact with Sgo1, we frequently isolated Par1—one of the PP2A-B56 homologues in fission yeast[28]. The interaction between Sgo1 and Par1 was confirmed by immunoprecipitation (Fig. 5a). In proliferating cells, Par1 localizes in the cytoplasm, and on the spindle pole body and the division septum (data not shown)[28,29]; however, it colocalizes with Sgo1 at centromeres during meiosis I (Fig. 5b). Sgo1 localization was not impaired in mutant *par1Δ* cells (data not shown). In contrast, the centromeric localization of Par1 was abolished in mutant *sgo1Δ* cells (Fig. 5c), indicative of the dependency of Par1 localization on shugoshin and reminiscent of the situation in human mitotic cells.

To examine whether Par1 is required for the protection of centromeric cohesin during meiosis, we analysed Rec8 localization at metaphase II—the period during which Rec8 is detected only at centromeres. We found that, like *sgo1Δ* cells, *par1Δ* cells mostly lost

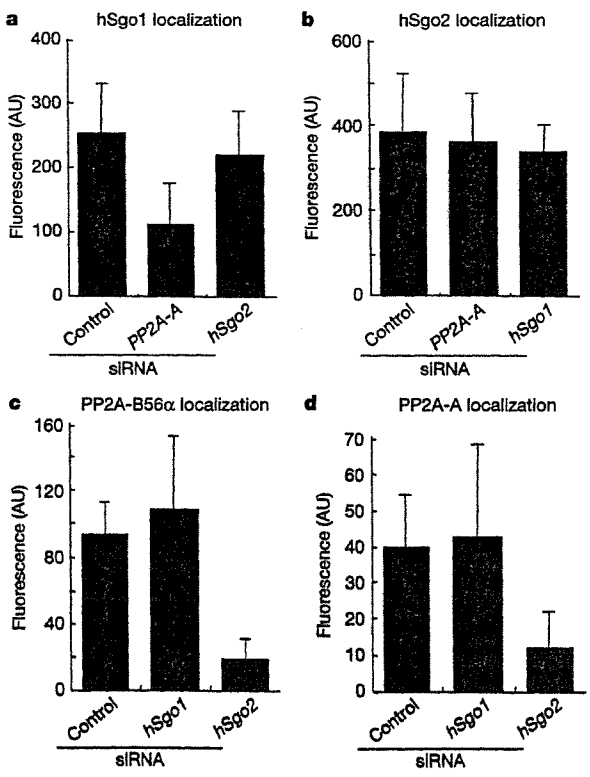

Figure 3 | Interdependency of shugoshin and PP2A for localization. **a–d**, Cells after siRNA treatment were stained with the indicated antibodies (**a**, hSgo1; **b**, hSgo2; **c**, PP2A-B56; **d**, PP2A-A; see also the representative stained cells in Supplementary Fig. 4). The intensities of the fluorescent centromeric signals in prometaphase cells were quantified as described in Methods. AU, arbitrary units. Error bars represent s.d. ($n = 20$).

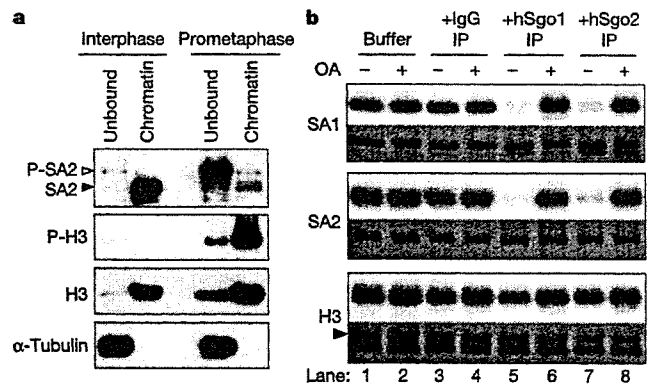

Figure 4 | Dephosphorylation of cohesin subunit SA. **a**, Chromatin-bound SA2 is dephosphorylated *in vivo*. Cell extracts prepared from interphase and prometaphase cells were fractionated into chromatin-bound and -unbound fractions and analysed by western blotting with the indicated antibodies. Four-times more of the chromatin-bound fractions were loaded. P-SA2, phosphorylated SA2; P-H3, histone H3 phosphorylated on Ser 10. In the mitotic chromatin-bound fraction, contaminated interphase chromatin is, if any, negligible (see Supplementary Fig. 9). **b**, Endogenous shugoshin associates with an okadaic-acid-inhibitable phosphatase activity that dephosphorylates cohesin subunit Scc3/SA. C-terminal peptides of SA1 or SA2 phosphorylated by Plk1, and a control histone H3 phosphorylated by Aurora B, were mixed with immunoprecipitation (IP) buffer (lane 1 and 2), control IgG immunoprecipitates (lane 3 and 4), immunoaffinity-purified hSgo1 (lane 5 and 6) or hSgo2 (lane 7 and 8) from HeLa cell extracts. Each sample was incubated in the presence (+) or absence (−) of 1 μM okadaic acid (OA) for 2 h. Autoradiography is shown in the upper panel, Coomassie blue staining in the lower panel.

centromeric Rec8 localization at this stage (Fig. 5d). Consistent with this observation, both of these mutant cell types showed precocious centromeric dissociation after meiosis I, and random chromosome segregation following meiosis II (Supplementary Fig. 7). *S. pombe* cells have another PP2A-B56 homologue, Par2, which is expressed at much lower levels[28] and contributes little to centromeric protection in meiosis (data not shown). Taken together, these results argue that, like Sgo1, Sgo1-associating PP2A (including Par1/PP2A-B56) has a crucial role in protecting cohesin at centromeres during meiosis I.

Individual protection ability of PP2A and shugoshin

Our current results in both human cells and fission yeast have raised the possibility that PP2A has an intrinsic ability to protect cohesin. Indeed, by ectopically localizing *S. pombe* Par1/PP2A-B56 to a specific site on a chromosome arm, we observed that the cohesion (and cohesin) at this site was partly preserved even after meiosis I—the period when arm cohesin should dissociate (Supplementary Fig. 8). To assess more thoroughly the individual ability of PP2A for centromeric protection, we used the 'ectopic protection system' in fission yeast, where coexpression of Rec8 and its protector blocks sister chromatid separation in mitosis, causing lethality[8]. We

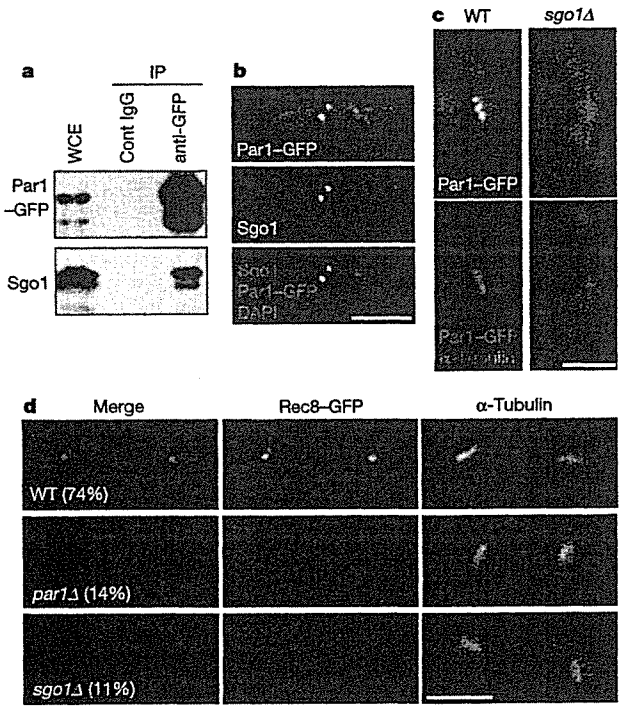

Figure 5 | *S. pombe* PP2A associating with Sgo1 is required for centromeric protection of Rec8-containing cohesin during meiosis I. **a**, Extracts, prepared from mitotic *par1*$^+$*–GFP* cells ectopically expressing Sgo1, were immunoprecipitated with control IgG or anti-GFP (green fluorescent protein) antibodies and analysed by western blotting using antibodies against GFP and Sgo1. WCE, 7.5% of the whole cell extract. **b**, Meiotic *par1*$^+$*–GFP* cells were arrested at metaphase I by repressing APC activation (*slp1*$^+$ and *cut23*$^+$ expression), and stained with DAPI (4,6-diamidino-2-phenylindole) and antibodies against Sgo1 and GFP. Colocalization was observed in most cells (95%, $n = 20$). **c**, As in **b**, fluorescence of Par1–GFP was examined at metaphase I in wild-type (WT) *sgo1*$^+$ and *sgo1Δ* cells. The spindles were visualized by expressing cyan fluorescent protein (CFP)–Atb2 (α2-tubulin). Par1–GFP was detected as dots in most metaphase I *sgo1*$^+$ cells (98%, $n = 219$), but never in *sgo1Δ* cells (0%, $n = 178$). **d**, The Rec8–GFP signal was monitored at prometaphase II in the indicated strains. Representative samples are shown together with the frequency of the cells showing centromeric Rec8–GFP ($n > 50$).

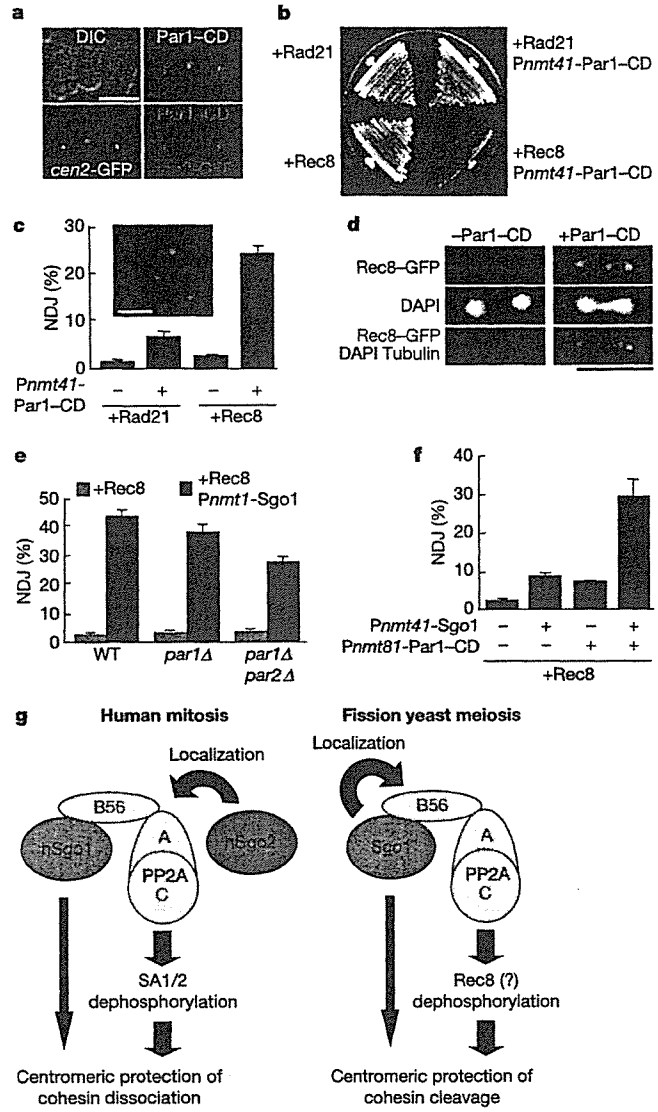

Figure 6 | Individual ability of PP2A and shugoshin for centromeric protection. **a**, Par1–CD proteins visualized by CFP localized in close vicinity to *cen2*-GFP in proliferating cells. **b**, The haploid *cen2-GFP* strains expressing the indicated genes by exogenous promoters (a constitutive promoter, P*adh1*, for *rad21*$^+$ and *rec8*$^+$, and a thiamine-repressible promoter, P*nmt41*, for *par1*$^+$*–CD*) were streaked on a thiamine-depleted plate. **c**, The strains in **b** were cultured at 30 °C for 15 h after thiamine depletion and the frequency of NDJ was counted among septated cells. Examples of *cen2*-GFP (green) in P*adh1-rec8*$^+$ P*nmt41-par1*$^+$*–CD* cells are shown. **d**, Centromeric Rec8–GFP signals are detected during anaphase in most *par1*$^+$*–CD*-expressing cells (81%) but in fewer non-expressing cells (19%). **e**, The indicated haploid *cen2-GFP* strains expressing Rec8 or Rec8 and Sgo1 (by the P*nmt1* promoter) were examined for the frequency of NDJ among septated cells. **f**, The haploid *cen2-GFP* P*adh1-rec8*$^+$ strains mildly expressing Sgo1 and/or Par1–CD were examined for the frequency of NDJ. Note the different strength of the thiamine repressible promoters (P*nmt1* > P*nmt41* > P*nmt81*). Error bars represent s.d. of triplicate samples (each $n > 100$) (**c**, **e**, **f**). Scale bars, 5 μm (**a**, **c**, **d**). **g**, Model for the collaboration of shugoshin and PP2A in protecting centromeric cohesin during human mitosis and fission yeast meiosis. PP2A containing the B56 subunit, which is recruited to the centromere by shugoshin (hSgo2 in human cells and Sgo1 in *S. pombe*), dephosphorylates cohesin subunits as a mechanism of protection. Human hSgo1 and *S. pombe* Sgo1 may have an individual activity for centromeric protection, apart from localizing PP2A to centromeres.

proposed that PP2A has an intrinsic ability to protect Rec8 without the help of Sgo1 once it is localized to centromeres. To test this, we endowed Par1 with its own ability to localize to centromeres by fusing its C-terminal end with the chromo domain (CD) of Swi6, which binds to Lys-9-methylated histone H3 largely locating at pericentromeric heterochromatin regions—the sites where Sgo1 usually localizes[8]. The engineered protein, Par1–CD, indeed localized at centromeres in mitotic cells in which Sgo1 is not expressed (Fig. 6a). Notably, coexpression of Par1–CD and Rec8 frequently led to blocked nuclear division, as centromere-associated *cen2*-GFP (green fluorescent protein) frequently segregated to the same side of a septated cell (Fig. 6b, c). This non-disjunction (NDJ) of sister chromatids presumably stems from persistent cohesion at anaphase because centromeric cohesin Rec8 was largely protected at this stage (Fig. 6d). Coexpression of Par1–CD with Rad21 caused a much weaker phenotype, indicative of the specificity of protection for the cohesin kleisin subunit (Fig. 6b, c). Finally, the protection is indeed executed by PP2A activity recruited by Par1–CD because the NDJ was suppressed by introducing a mutation in Ppa2, a major catalytic subunit of PP2A in fission yeast[30] (NDJ decreased from 24% to 7%). As Sgo1 is meiosis-specific and is not expressed in mitotic cells, these results demonstrate that centromeric localization of PP2A itself can protect Rec8 cohesin from cleavage, suggesting that dephosphorylation of cohesin Rec8 is a mechanism for the protection of sister centromeres in fission yeast.

We noticed that the ectopic protection mediated by Sgo1 overexpression was alleviated, but not abolished, when endogenous Par1 (or both Par1 and Par2) was depleted from the cells (Fig. 6e). This indicates that Sgo1 also has an individual ability to protect Rec8-containing cohesin without the aid of PP2A-B56 if sufficient amounts of protein are expressed. However, in physiological meiosis, this ability of Sgo1 is not sufficient to complement the loss of PP2A activity. The collaboration of Sgo1 and PP2A was further supported by the observation that coexpression of Sgo1 and Par1–CD mediated a synergistic effect on centromeric protection (Fig. 6f).

Discussion

In animal cells, most cohesin is removed from chromosome arms during prophase and prometaphase, triggered by Plk1-dependent phosphorylation of the Scc3/SA subunit of cohesin[17]. Here we have discovered that a B56-containing subtype of PP2A phosphatase associates with hSgo1 in human cells, playing a crucial part in preventing cohesin dissociation at centromeres. We have also demonstrated that chromatin-bound SA2 at centromeres is mostly dephosphorylated in prometaphase cells, whereas dissociated SA2 from the arms is phosphorylated (Fig. 4a). Furthermore, purified hSgo1 or hSgo2 complex can counteract Plk1-dependent SA phosphorylation *in vitro* (Fig. 4b). Thus, our results argue that dephosphorylation of Scc3/SA by shugoshin-associating PP2A is a mechanism for centromeric protection (Fig. 6g). Because dephosphorylated SA2 is detected only in the chromatin-bound fraction of cohesin, we suggest that the regulation takes place exactly at the sites where shugoshin–PP2A complexes localize. Previous results suggested that Plk-dependent phosphorylation of Scc1/Rad21 facilitates its cleavage by separase but is not essential[17,19,20], whereas phosphorylation of Rec8 might be crucial for cleavage[21,22]. Here we have demonstrated that *S. pombe* Par1/PP2A-B56 associating with Sgo1 is required and even sufficient for protecting cohesin Rec8 from separase cleavage. Moreover, PP2A-dependent cohesin protection requires the kleisin subunit Rec8 (Fig. 6b, c), suggesting that the extent of phosphorylation and/or its contribution to the susceptibility to separase cleavage is different between Scc1/Rad21 and Rec8. These results are consistent with the notion that PP2A activity counteracts the phosphorylation of Rec8, thereby protecting it from separase cleavage during meiosis I. Chromosome segregation in mouse meiosis is also disturbed by okadaic acid treatment, which results in premature separation of sister chromatids during meiosis I[31]. Thus, the shugoshin–PP2A system found in *S. pombe* meiosis is presumably applicable to mammalian meiosis. Taken together, centromeric protection of eukaryotic chromosomes may be executed at the level of dephosphorylation of cohesin subunits, and a subtype of PP2A containing the B56 subunit has a direct role in this process. This concept is applicable for both mitosis and meiosis, albeit the crucial target of dephosphorylation is different, being Scc3/SA in mitosis and Rec8 in meiosis (Fig. 6g).

The depletion of hSgo1 by siRNA caused precocious separation of centromeric cohesion (Fig. 2), although the centromeric localization of PP2A is preserved (Fig. 3c, d), suggesting that protection is not solely executed by linking PP2A to centromeres. Moreover, *hSgo2* siRNA caused fewer defects in protection than *hSgo1* siRNA (Fig. 2e). Therefore, hSgo2 might solely be required to tether PP2A to centromeres, whereas—besides facilitating PP2A function at centromeres—hSgo1 might have an additional role in protection (Fig. 6g). Supporting this notion, ectopic expression of *S. pombe* Sgo1 and Rec8 can enforce centromeric protection even in PP2A-B56-depleted cells (Fig. 6e). Because shugoshin closely associates with cohesin *in vivo*[8,12,32], we favour the possibility that Sgo1 physically protects cohesin against access by an inactivating enzyme (for example, Plk1 in human mitosis and Plk or separase in fission yeast meiosis). As Plk is suggested to phosphorylate and delocalize Sgo/MEI-S332 in *Drosophila*[33], PP2A might facilitate the localization of shugoshin, which is supported by our observation that hSgo1 localization partly depends on PP2A (Fig. 3a). Thus, shugoshin and PP2A may support each other, collaboratively protecting cohesin at centromeres. *S. pombe* Sgo1 has roles in both recruiting PP2A and protecting cohesin *per se* at centromeres. In contrast, hSgo1 is dispensable for localizing PP2A to centromeres but is required for centromeric protection, whereas hSgo2 is required for the recruitment of PP2A to centromeres, implying a 'division of labour' between these two shugoshin-like proteins in human cells. Thus, the interplay of shugoshin and PP2A is apparently conserved across human and fission yeast, or mitosis and meiosis (Fig. 6g).

PP2A is a family of abundantly expressed protein phosphatases, the activity of which is highly regulated and implicated in a multitude of cellular processes, such as signal transduction, development and tumorigenesis[34]. Chromosome mis-segregation in mitosis may contribute to tumorigenesis. Meiotic chromosome segregation is also important clinically, as failures in this process cause birth defects in humans. Our study may provide a novel link between PP2A and tumorigenesis or birth defects, and therefore is useful for future studies in those fields as well.

METHODS

Antibody production and immunofluorescence microscopy. Antibody production and immunofluorescence staining were performed as described in Supplementary Methods.

Quantification of fluorescent signals. To quantify the centromeric fluorescent signals, in-focus images of the cyclin B1-or phospho-H3-positive prometaphase cells were taken with the use of MetaMorph imaging software (Universal Imaging). We measured the maximum intensity among the centromeric signals within the cell and subtracted the background intensity of the region, which was measured directly adjacent to the centromere.

RNA interference. Synthetic sense and antisense siRNA oligonucleotides for *hSgo1* (ref. 14) and *hSgo2* (5′-GCACUACCACUUUGAAUAATT-3′), *PP2A-Aα* (5′-AGACUUGACAUGUUGGUUGTT-3′) and *PP2A-Aβ* (5′-UUUCUACUCC AAGUGCUAGTT-3′) were obtained from JbioS. Note that PP2A-B56 consists of five isoforms, whereas the PP2A-A core subunit has only two isoforms. Therefore, we constructed siRNAs against PP2A-A isoforms, rather than PP2A-B56 isoforms, to reduce PP2A activity. The presented data were obtained using the abovementioned siRNAs, but we confirmed that similar results were obtained by using another set of siRNAs: *hSgo2* (5′-GCUCUCAUGAACAAUAACUTT-3′), *PP2A-Aα* (5′-GCAUCAAUGUGCUGUCUGATT-3′) and *PP2A-Aβ* (5′-CGAC UCAACAGUAUUAAGATT-3′). Cells at 20% confluency in Opti-MEM medium (Invitrogen) were transfected with siRNA duplexes at a final concentration of 400 nM and Oligofectamine (Invitrogen) at 1:250, and complete medium containing 20% FBS was added at 1:1 after 6 h. After two days incubation, the

cells were examined. All control samples were similarly treated but were exposed to H_2O instead of siRNA reagent.

Preparation of HeLa cell extracts. Preparation of HeLa cell extracts and subsequent immunoprecipitation or fractionation are described in Supplementary Methods.

***In vitro* dephosphorylation assay.** To generate phosphorylated SA substrates, a 6× His-tagged SA1 C-terminal peptide (amino acids 923–1258) or SA2 C-terminal peptide (amino acids 895–1232) was expressed in *Escherichia coli* strain BL21 and purified with Ni-NTA agarose (Qiagen), and labelled with [γ-^{32}P]ATP using recombinant Plk1 kinase (ref. 35). As a control, core histone proteins were labelled with [γ-^{32}P]ATP by recombinant Aurora B kinase. The immunoprecipitated complexes from HeLa cell extracts were collected after washing with immunoprecipitation buffer without phosphatase inhibitors (20 mM Tris-HCl, pH 7.5, 100 mM NaCl, 0.1% Tween 20, 10% glycerol and 10 mM β-mercaptoethanol). The equivalent of 3 μl of immunoprecipitated beads was preincubated with 1 μM of okadaic acid or dimethylsulphoxide (DMSO) for 20 min at room temperature (~20 °C), followed by the addition of ^{32}P-labelled SA substrates in a dephosphorylation buffer (50 mM Tris-HCl, pH 7.5, 100 mM NaCl, 0.01% Brij35, 2 mM $MnCl_2$, 0.1 mM EGTA, 2 mM dithiothreitol (DTT)) supplemented with 1 μg of BSA to a total reaction volume of 15 μl and incubated for 2 h at 30 °C with gentle agitation.

Chromosome spreading. Mitotic HeLa cells were collected by mitotic shake-off and treated with 330 nM nocodazole for 4 h. Chromosome spreading was performed as described previously[36].

Yeast experiments. All *S. pombe* strains used are listed in Supplementary Table 1. General methods for immunoprecipitation, culturing *S. pombe*, inducing meiosis and monitoring chromosome segregation were as described previously[8]. Further details of *S. pombe* experiments, as well as the yeast two-hybrid assay, are described in Supplementary Methods.

Received 3 October 2005; accepted 21 February 2006.
Published online 15 March 2006.

1. Nasmyth, K. Disseminating the genome: joining, resolving, and separating sister chromatids during mitosis and meiosis. *Annu. Rev. Genet.* **35**, 673–745 (2001).
2. Milutinovich, M. & Koshland, D. E. SMC complexes–wrapped up in controversy. *Science* **300**, 1101–1102 (2003).
3. Hirano, T. Dynamic molecular linkers of the genome: the first decade of SMC proteins. *Genes Dev.* **19**, 1269–1287 (2005).
4. Hauf, S. & Watanabe, Y. Kinetochore orientation in mitosis and meiosis. *Cell* **119**, 317–327 (2004).
5. Uhlmann, F. Chromosome cohesion and separation: from men and molecules. *Curr. Biol.* **13**, R104–R114 (2003).
6. Lee, J. Y. & Orr-Weaver, T. L. The molecular basis of sister-chromatid cohesion. *Annu. Rev. Cell Dev. Biol.* **17**, 753–777 (2001).
7. Watanabe, Y. Shugoshin: guardian spirit at the centromere. *Curr. Opin. Cell Biol.* **17**, 590–595 (2005).
8. Kitajima, T. S., Kawashima, S. A. & Watanabe, Y. The conserved kinetochore protein shugoshin protects centromeric cohesion during meiosis. *Nature* **427**, 510–517 (2004).
9. Rabitsch, K. P. *et al.* Two fission yeast homologs of *Drosophila Mei-S332* are required for chromosome segregation during meiosis I and II. *Curr. Biol.* **14**, 287–301 (2004).
10. Marston, A. L., Tham, W. H., Shah, H. & Amon, A. A genome-wide screen identifies genes required for centromeric cohesion. *Science* **303**, 1367–1370 (2004).
11. Katis, V. L., Galova, M., Rabitsch, K. P., Gregan, J. & Nasmyth, K. Maintenance of cohesin at centromeres after meiosis I in budding yeast requires a kinetochore-associated protein related to MEI-S332. *Curr. Biol.* **14**, 560–572 (2004).
12. Hamant, O. *et al.* A REC8-dependent plant shugoshin is required for maintenance of centromeric cohesion during meiosis and has no mitotic functions. *Curr. Biol.* **15**, 948–954 (2005).
13. Salic, A., Waters, J. C. & Mitchison, T. J. Vertebrate shugoshin links sister centromere cohesion and kinetochore microtubule stability in mitosis. *Cell* **118**, 567–578 (2004).
14. Kitajima, T. S., Hauf, S., Ohsugi, M., Yamamoto, T. & Watanabe, Y. Human Bub1 defines the persistent cohesion site along the mitotic chromosome by affecting Shugoshin localization. *Curr. Biol.* **15**, 353–359 (2005).
15. McGuinness, B. E., Hirota, T., Kudo, N. R., Peters, J.-M. & Nasmyth, K. Shugoshin prevents dissociation of cohesin from centromeres during mitosis in vertebrate cells. *PLoS Biol.* **3**, e86 (2005).
16. Sumara, I. *et al.* The dissociation of cohesin from chromosomes in prophase is regulated by Polo-like kinase. *Mol. Cell* **9**, 515–525 (2002).
17. Hauf, S. *et al.* Dissociation of cohesin from chromosome arms and loss of arm cohesion during early mitosis depends on phosphorylation of SA2. *PLoS Biol.* **3**, e69 (2005).
18. Losada, A., Hirano, M. & Hirano, T. Cohesin release is required for sister chromatid resolution, but not for condensin-mediated compaction, at the onset of mitosis. *Genes Dev.* **16**, 3004–3016 (2002).
19. Alexandru, G., Uhlmann, F., Mechtler, K., Poupart, M. & Nasmyth, K. Phosphorylation of the cohesin subunit Scc1 by Polo/Cdc5 kinase regulates sister chromatid separation in yeast. *Cell* **105**, 459–472 (2001).
20. Hornig, N. C. & Uhlmann, F. Preferential cleavage of chromatin-bound cohesin after targeted phosphorylation by Polo-like kinase. *EMBO J.* **23**, 3144–3153 (2004).
21. Lee, B. H. & Amon, A. Role of Polo-like kinase *CDC5* in programming meiosis I chromosome segregation. *Science* **300**, 482–486 (2003).
22. Clyne, R. K. *et al.* Polo-like kinase Cdc5 promotes chiasmata formation and cosegregation of sister centromeres at meiosis I. *Nature Cell Biol.* **5**, 480–485 (2003).
23. Natsume, T. *et al.* A direct nanoflow liquid chromatography–tandem mass spectrometry system for interaction proteomics. *Anal. Chem.* **74**, 4725–4733 (2002).
24. Janssens, V. & Goris, J. Protein phosphatase 2A: a highly regulated family of serine/threonine phosphatases implicated in cell growth and signalling. *Biochem. J.* **353**, 417–439 (2001).
25. Tang, Z., Sun, Y., Harley, S. E., Zou, H. & Yu, H. Human Bub1 protects centromeric sister-chromatid cohesion through Shugoshin during mitosis. *Proc. Natl Acad. Sci. USA* **101**, 18012–18017 (2004).
26. Vandre, D. D. & Wills, V. L. Inhibition of mitosis by okadaic acid: possible involvement of a protein phosphatase 2A in the transition from metaphase to anaphase. *J. Cell Sci.* **101**, 79–91 (1992).
27. Van Dolah, F. M. & Ramsdell, J. S. Okadaic acid inhibits a protein phosphatase activity involved in formation of the mitotic spindle of GH4 rat pituitary cells. *J. Cell. Physiol.* **152**, 190–198 (1992).
28. Jiang, W. & Hallberg, R. L. Isolation and characterization of *par1*$^+$ and *par2*$^+$: two *Schizosaccharomyces pombe* genes encoding B′ subunits of protein phosphatase 2A. *Genetics* **154**, 1025–1038 (2000).
29. Le Goff, X. *et al.* The protein phosphatase 2A B′-regulatory subunit par1p is implicated in regulation of the *S. pombe* septation initiation network. *FEBS Lett.* **508**, 136–142 (2001).
30. Kinoshita, N., Ohkura, H. & Yanagida, M. Distinct, essential roles of type 1 and 2A protein phosphatases in control of the fission yeast cell division cycle. *Cell* **63**, 405–415 (1990).
31. Mailhes, J. B., Hilliard, C., Fuseler, J. W. & London, S. N. Okadaic acid, an inhibitor of protein phosphatase 1 and 2A, induces premature separation of sister chromatids during meiosis I and aneuploidy in mouse oocytes *in vitro*. *Chromosome Res.* **11**, 619–631 (2003).
32. Kiburz, B. M. *et al.* The core centromere and Sgo1 establish a 50-kb cohesin-protected domain around centromeres during meiosis I. *Genes Dev.* **19**, 3017–3030 (2005).
33. Clarke, A. S., Tang, T. T., Ooi, D. L. & Orr-Weaver, T. L. POLO kinase regulates the *Drosophila* centromere cohesion protein MEI-S332. *Dev. Cell* **8**, 53–64 (2005).
34. Janssens, V., Goris, J. & Van Hoof, C. PP2A: the expected tumor suppressor. *Curr. Opin. Genet. Dev.* **15**, 34–41 (2005).
35. Nakajima, H., Toyoshima-Morimoto, F., Taniguchi, E. & Nishida, E. Identification of a consensus motif for Plk (Polo-like kinase) phosphorylation reveals Myt1 as a Plk1 substrate. *J. Biol. Chem.* **278**, 25277–25280 (2003).
36. Hauf, S. *et al.* The small molecule Hesperadin reveals a role for Aurora B in correcting kinetochore–microtubule attachment and in maintaining the spindle assembly checkpoint. *J. Cell Biol.* **161**, 281–294 (2003).

Supplementary Information is linked to the online version of the paper at www.nature.com/nature.

Acknowledgements We thank S. Hauf for critically reading the manuscript. We also thank B. Akiyoshi for yeast two-hybrid screening of *S. pombe* Sgo1; K. Nasmyth for communicating unpublished results; J. M. Peters, E. Nishida, F. Ishikawa, Y. Nakatani, M. Sato and T. Toda for reagents; J. M. Peters, M. Ohsugi and M. Shimura for methods; and all members in our laboratory for their valuable discussion and help. K.I. was supported by a JSPS fellowship. This work was supported in part by the New Energy and Industrial Technology Development Organization (to T.N.), and by the Toray Science Foundation, Uehara Memorial Foundation, and a Grant-in-Aid for Specially Promoted Research from the Ministry of Education, Culture, Sports, Science and Technology of Japan (to Y.W.).

Author Contributions Experiments in Figs 1–3 were mainly performed by T.S.K., Fig. 4 by K.I., and Figs 5 and 6 by T.S. and S.A.K. Mass spectrometry of hSgo1 immunoprecipitates was performed by S.I. and T.N. Experimental design, interpretation of data, and the preparation of the manuscript were mainly conducted by T.S.K., T.S., K.I. and Y.W.

Author Information Reprints and permissions information is available at npg.nature.com/reprintsandpermissions. The authors declare no competing financial interests. Correspondence and requests for materials should be addressed to Y.W. (ywatanab@iam.u-tokyo.ac.jp).

Brief Genetics Report

Association Studies of Variants in the Genes Involved in Pancreatic β-Cell Function in Type 2 Diabetes in Japanese Subjects

Norihide Yokoi,[1] Masao Kanamori,[2] Yukio Horikawa,[3] Jun Takeda,[3] Tokio Sanke,[4] Hiroto Furuta,[5] Kishio Nanjo,[5] Hiroyuki Mori,[6] Masato Kasuga,[6] Kazuo Hara,[7] Takashi Kadowaki,[7] Yukio Tanizawa,[8] Yoshitomo Oka,[9] Yukiko Iwami,[10] Hisako Ohgawara,[10] Yuichiro Yamada,[11] Yutaka Seino,[11] Hideki Yano,[12] Nancy J. Cox,[13] and Susumu Seino[1]

Because impaired insulin secretion is characteristic of type 2 diabetes in Asians, including Japanese, the genes involved in pancreatic β-cell function are candidate susceptibility genes for type 2 diabetes. We examined the association of variants in genes encoding several transcription factors (*TCF1*, *TCF2*, *HNF4A*, *ISL1*, *IPF1*, *NEUROG3*, *PAX6*, *NKX2–2*, *NKX6–1*, and *NEUROD1*) and genes encoding the ATP-sensitive K^+ channel subunits Kir6.2 (*KCNJ11*) and SUR1 (*ABCC8*) with type 2 diabetes in a Japanese cohort of 2,834 subjects. The exon 16 −3c/t variant rs1799854 in *ABCC8* showed a significant association ($P = 0.0073$), and variants in several genes showed nominally significant associations ($P < 0.05$) with type 2 diabetes. Although the E23K variant rs5219 in *KCNJ11* showed no association with diabetes in Japanese (for the K allele, odds ratio [OR] 1.08 [95% CI 0.97–1.21], $P = 0.15$), 95% CI around the OR overlaps in meta-analysis of European populations, suggesting that our results are not inconsistent with the previous studies. This is the largest association study so far conducted on these genes in Japanese and provides valuable information for comparison with other ethnic groups. *Diabetes* 55:2379–2386, 2006

Impaired insulin secretion and insulin resistance both contribute to the pathogenesis of type 2 diabetes. The former is a characteristic feature of type 2 diabetes, especially in Asians including Japanese (1), and genes encoding proteins critical in pancreatic β-cell function are therefore particularly good candidate susceptibility genes for type 2 diabetes for this population. Studies of maturity-onset diabetes of the young in humans (2) and knockout mice (3) have shown that mutations of transcription factors required for development, differentiation, and maintenance of the pancreatic β-cells can cause diabetes. Pancreatic β-cell ATP-sensitive K^+ channels (K_{ATP} channels) are crucial in the regulation of insulin secretion by coupling cell metabolism to membrane electrical activity. The pancreatic β-cell K_{ATP} channel comprises two subunits, the inwardly rectifying potassium channel Kir6.2 (*KCNJ11*) and the sulfonylurea receptor SUR1 (*ABCC8*) (4). Mutations in the genes (*ABCC8* and *KCNJ11*) can cause familial persistent hyperinsulinemic hypoglycemia of infancy (5) and permanent neonatal diabetes (6). Several polymorphisms in these genes also have been reported to be associated with type 2 diabetes in populations with distinct ethnic backgrounds (7–20). However, a large-scale association study of these genes has not been performed in type 2 diabetes in the Japanese population. Here, we report on the association of variants in genes encoding various transcription factors and pancreatic β-cell K_{ATP} channel subunits with type 2 diabetes in a large Japanese cohort.

A case-control association study using 1,590 Japanese diabetic subjects and 1,244 nondiabetic control subjects was performed. All subjects were genotyped for 33 variants of 12 genes including transcription factors (*TCF1*, *TCF2*, *HNF4A*, *ISL1*, *IPF1*, *NEUROG3*, *PAX6*, *NKX2–2*, *NKX6–1*, and *NEUROD1*) and β-cell K_{ATP} channel subunits (*KCNJ11* and *ABCC8*) (Table 1).

Results of Hardy-Weinberg equilibrium (HWE) tests are shown in Table 1 of the online appendix (available at http://diabetes.diabetesjournals.org). All genotypes were in HWE, except for departures in cases at *TCF2*_SNP (single nucleotide polymorphism) 5 rs2689, *TCF2*_SNP6

From the [1]Division of Cellular and Molecular Medicine, Kobe University Graduate School of Medicine, Kobe, Japan; the [2]Division of Health and Preventive Medicine, Department of Lifelong Sport, Biwako Seikei Sport College, Shiga, Japan; the [3]Department of Endocrinology, Diabetes and Rheumatology, Division of Bioregulatory Medicine, Gifu University School of Medicine, Gifu, Japan; the [4]Department of Clinical Laboratory Medicine, Wakayama University of Medical Science, Wakayama, Japan; the [5]First Department of Medicine, Wakayama University of Medical Science, Wakayama, Japan; the [6]Department of Clinical Molecular Medicine, Division of Diabetes and Digestive and Kidney Diseases, Kobe University Graduate School of Medicine, Kobe, Japan; the [7]Department of Metabolic Diseases, Graduate School of Medicine, University of Tokyo, Tokyo, Japan; the [8]Division of Molecular Analysis of Human Disorders, Department of Bio-Signal Analysis, Yamaguchi University Graduate School of Medicine, Ube, Japan; the [9]Division of Molecular Metabolism and Diabetes, Tohoku University Graduate School of Medicine, Sendai, Japan; the [10]Division of Cell Replacement and Regenerative Medicine, Medical Research Institute, School of Medicine, Tokyo Women's Medical University, Tokyo, Japan; the [11]Department of Diabetes and Clinical Nutrition, Kyoto University Graduate School of Medicine, Kyoto, Japan; the [12]Department of Internal Medicine, Hikone Municipal Hospital, Shiga, Japan; and the [13]Departments of Medicine and Human Genetics, University of Chicago, Chicago, Illinois.

Address correspondence and reprint requests to Susumu Seino, Division of Cellular and Molecular Medicine, Kobe University Graduate School of Medicine, Chuo-ku, Kobe 650-0017, Japan. E-mail: seino@med.kobe-u.ac.jp.

Received for publication 13 September 2005 and accepted in revised form 22 May 2006.

Additional information for this article can be found in an online appendix at http://diabetes.diabetesjournals.org.

HWE, Hardy-Weinberg equilibrium; K_{ATP} channel, ATP-sensitive K^+ channel; LD, linkage disequilibrium; SNP, single nucleotide polymorphism.

DOI: 10.2337/db05-1203

TABLE 1
Summary of association studies of 33 variants for 12 genes with type 2 diabetes

Number	Locus	HapMap data	Subject	Allele data (frequency) 1	Allele data (frequency) 3	Genotype data (frequency) 1	Genotype data (frequency) 2	Genotype data (frequency) 3	*P* value Allele 2*2	*P* value Genotype 2*3	OR (95% CI)
1	TCF1_SNP1			A	C	A/A	A/C	C/C			
	rs1169288	JPT	Case	1,590 (0.50)	1,590 (0.50)	385 (0.24)	820 (0.52)	385 (0.24)	0.4508	0.2388	1.04 (0.94–1.16)
	I27L		Control	1,270 (0.51)	1,218 (0.49)	332 (0.27)	606 (0.49)	306 (0.25)			
2	TCF1_SNP2			G	A	G/G	G/A	A/A			
	rs1169294	none	Case	1,702 (0.54)	1,478 (0.46)	443 (0.28)	816 (0.51)	331 (0.21)	0.3247	0.1566	1.06 (0.95–1.17)
	IVS1 −42		Control	1,298 (0.52)	1,190 (0.48)	348 (0.28)	602 (0.48)	294 (0.24)			
3	TCF1_SNP3			A	T	A/A	A/T	T/T			
	rs2071190	JPT	Case	482 (0.15)	2,698 (0.85)	38 (0.02)	406 (0.26)	1,146 (0.72)	0.8925	0.8617	1.01 (0.87–1.17)
	IVS2 −51		Control	373 (0.15)	2,115 (0.85)	26 (0.02)	321 (0.26)	897 (0.72)			
4	TCF2_SNP1			G	A	G/G	G/A	A/A			
	rs757210	JPT	Case	2,079 (0.65)	1,101 (0.35)	697 (0.44)	685 (0.43)	208 (0.13)	0.4565	0.2695	1.04 (0.93–1.17)
	IVS2 + 2916		Control	1,651 (0.66)	837 (0.34)	546 (0.44)	559 (0.45)	139 (0.11)			
5	TCF2_SNP2			A	G	A/A	A/G	G/G			
	rs757211	none	Case	1,460 (0.46)	1,720 (0.54)	342 (0.22)	776 (0.49)	472 (0.30)	0.6994	0.5473	1.02 (0.92–1.14)
	IVS2 + 2953		Control	1,156 (0.46)	1,332 (0.54)	262 (0.21)	632 (0.51)	350 (0.28)			
6	TCF2_SNP3			G	A	G/G	G/A	A/A			
	rs718960	JPT	Case	2,288 (0.72)	892 (0.28)	824 (0.52)	640 (0.40)	126 (0.08)	0.6121	0.8597	1.03 (0.92–1.16)
	IVS4 + 14307		Control	1,774 (0.71)	714 (0.29)	632 (0.51)	510 (0.41)	102 (0.08)			
7	TCF2_SNP4			T	A	T/T	T/A	A/A			
	rs1016991	JPT	Case	2,823 (0.89)	357 (0.11)	1,260 (0.79)	303 (0.19)	27 (0.02)	0.0105*	0.0399*	1.23 (1.05–1.45)
	IVS8 + 929		Control	2,152 (0.87)	336 (0.14)	938 (0.75)	276 (0.22)	30 (0.02)			
8	TCF2_SNP5			A	T	A/A	A/T	T/T			
	rs2689	JPT	Case	1,722 (0.54)	1,458 (0.46)	488 (0.31)	746 (0.47)	356 (0.22)	0.5195	0.3582	1.04 (0.93–1.15)
	+274 TGA		Control	1,325 (0.53)	1,163 (0.47)	355 (0.29)	615 (0.49)	274 (0.22)			
9	TCF2_SNP6			A	C	A/A	A/C	C/C			
	rs2688	JPT	Case	1,840 (0.58)	1,340 (0.42)	552 (0.35)	736 (0.46)	302 (0.19)	0.0563	0.0291*	1.11 (1.00–1.24)

	+444 TGA		Control	1,503 (0.60)	985 (0.40)	448 (0.36)	607 (0.49)	189 (0.15)			
10	HNF4A_SNP1			T	C	T/T	T/C	C/C			
	rs717247	JPT	Case	2,277 (0.72)	903 (0.28)	811 (0.51)	655 (0.41)	124 (0.08)	0.2071	0.4223	1.08 (0.96–1.22)
	−4229		Control	1,820 (0.73)	668 (0.27)	661 (0.53)	498 (0.40)	85 (0.07)			
11	HNF4A_SNP2			A	G	A/A	A/G	G/G			
	rs736820	none	Case	1,207 (0.38)	1,973 (0.62)	230 (0.14)	747 (0.47)	613 (0.39)	0.4482	0.6472	1.04 (0.94–1.16)
	IVS1 + 3889		Control	919 (0.37)	1,569 (0.63)	176 (0.14)	567 (0.46)	501 (0.40)			
12	HNF4A_SNP3			T	C	T/T	T/C	C/C			
	rs745975	JPT	Case	643 (0.20)	2,537 (0.80)	53 (0.03)	537 (0.34)	1,000 (0.63)	0.0470*	0.0769	1.15 (1.00–1.31)
	IVS1 −5		Control	450 (0.18)	2,038 (0.82)	39 (0.03)	372 (0.30)	833 (0.67)			
13	ISL1_SNP10			G	A	G/G	G/A	A/A			
	rs2303750	none	Case	2,842 (0.89)	338 (0.11)	1,271 (0.80)	300 (0.19)	19 (0.01)	0.5101	0.4453	1.06 (0.90–1.26)
	IVS3 −4		Control	2,209 (0.89)	279 (0.11)	987 (0.79)	235 (0.19)	22 (0.02)			
14	ISL1_SNP11			A	G	A/A	A/G	G/G			
	rs2303751	none	Case	2,466 (0.78)	714 (0.22)	958 (0.60)	550 (0.35)	82 (0.05)	0.0539	0.1224	1.14 (1.00–1.29)
	P165P		Control	1,983 (0.80)	505 (0.20)	787 (0.63)	409 (0.33)	48 (0.04)			
15	IPF1_SNP3			G	T	G/G	G/T	T/T			
	rs4430606	none	Case	1,688 (0.53)	1,492 (0.47)	451 (0.28)	786 (0.49)	353 (0.22)	0.1807	0.3405	1.06 (0.90–1.26)
	IVS1 + 512		Control	1,366 (0.55)	1,122 (0.45)	371 (0.30)	624 (0.50)	249 (0.20)			
16	IPF1_SNP4			A	C	A/A	A/C	C/C			
	rs1124607	JPT	Case	2,527 (0.79)	653 (0.21)	1,007 (0.63)	513 (0.32)	70 (0.04)	0.7609	0.6259	1.02 (0.90–1.16)
	IVS1 + 539		Control	1,968 (0.79)	520 (0.21)	788 (0.63)	392 (0.32)	64 (0.05)			
17	IPF1_SNP7			G	A	G/G	G/A	A/A			
	none	none	Case	2,836 (0.89)	344 (0.11)	1,260 (0.79)	316 (0.20)	14 (0.01)	0.1309	0.2318	1.14 (0.97–1.34)
	IVS1 + 1787		Control	2,186 (0.88)	302 (0.12)	953 (0.77)	280 (0.23)	11 (0.01)			

Continued on following page

TABLE 1
Continued

Number	Locus	HapMap data	Subject	Allele data (frequency) 1	Allele data (frequency) 3	Genotype data (frequency) 1	Genotype data (frequency) 2	Genotype data (frequency) 3	*P* value Allele 2*2	*P* value Genotype 2*3	OR (95% CI)
18	NEUROG3_SNP1			A	G	A/A	A/G	G/G			
	rs3812704	JPT	Case	1,472 (0.46)	1,708 (0.54)	337 (0.21)	798 (0.50)	455 (0.29)	0.2674	0.4687	1.06 (0.96–1.18)
	−1822		Control	1,114 (0.45)	1,374 (0.55)	252 (0.20)	610 (0.49)	382 (0.31)			
19	NEUROG3_SNP2			T	C	T/T	T/C	C/C			1.06 (0.95–1.19)
	rs4536103	JPT	Case	2,268 (0.71)	912 (0.29)	798 (0.50)	672 (0.42)	120 (0.08)	0.3129	0.2040	
	F199S		Control	1,743 (0.70)	745 (0.30)	616 (0.50)	511 (0.41)	117 (0.09)			
20	PAX6_SNP1			A	T	A/A	A/T	T/T			1.08 (0.97–1.20)
	rs2239789	none	Case	1,725 (0.54)	1,455 (0.46)	483 (0.30)	759 (0.48)	348 (0.22)	0.1697	0.2391	
	IVS6 + 282		Control	1,396 (0.56)	1,092 (0.44)	392 (0.32)	612 (0.49)	240 (0.19)			
21	PAX6_SNP2			C	T	C/C	C/T	T/T			1.01 (0.86–1.18)
	rs667773	none	Case	2,791 (0.88)	389 (0.12)	1,228 (0.77)	335 (0.21)	27 (0.02)	0.9358	0.8923	
	IVS7 + 218		Control	2,181 (0.88)	307 (0.12)	961 (0.77)	259 (0.21)	24 (0.02)			
22	NKX2-2_SNP1			T	C	T/T	T/C	C/C			1.08 (0.74–1.56)
	none	none	Case	3,117 (0.98)	63 (0.02)	1,530 (0.96)	57 (0.04)	3 (0.002)	0.7650	0.8727	
	+856 TGA		Control	2,435 (0.98)	53 (0.02)	1,193 (0.96)	49 (0.04)	2 (0.002)			
23	NKX2-2_SNP2			C	T	C/C	C/T	T/T			1.13 (1.02–1.25)
	rs3746741	none	Case	1,666 (0.52)	1,514 (0.48)	452 (0.28)	762 (0.48)	376 (0.24)	0.0251*	0.0563	
	+1163 TGA		Control	1,228 (0.49)	1,260 (0.51)	305 (0.25)	618 (0.50)	321 (0.26)			
24	NKX6-1_SNP1			A	C	A/A	A/C	C/C			1.03 (0.92–1.16)
	rs1017560	JPT	Case	2,182 (0.69)	998 (0.31)	747 (0.47)	688 (0.43)	155 (0.10)	0.6052	0.0144*	
	−15606		Control	1,724 (0.69)	764 (0.31)	625 (0.50)	474 (0.38)	145 (0.12)			
25	NKX6-1_SNP2			T	G	T/T	T/G	G/G			1.01 (0.83–1.23)
	none	none	Case	2,939 (0.92)	241 (0.08)	1,359 (0.85)	221 (0.14)	10 (0.01)	0.9750	0.9966	
	−8823		Control	2,298 (0.92)	190 (0.08)	1,062 (0.85)	174 (0.14)	8 (0.01)			

26	NKX6-1_SNP3			G	A	G/G	G/A	A/A			1.05 (0.95–1.17)
	rs1545330	JPT	Case	1,719 (0.54)	1,461 (0.46)	452 (0.28)	815 (0.51)	323 (0.20)	0.3348	0.5938	
	−8797		Control	1,312 (0.53)	1,176 (0.47)	338 (0.27)	636 (0.51)	270 (0.22)			
27	NKX6-1_SNP4			A	C	A/A	A/C	C/C			1.01 (0.90–1.13)
	rs2278671	JPT	Case	2,094 (0.66)	1,086 (0.34)	681 (0.43)	732 (0.46)	177 (0.11)	0.8884	0.5354	
	IVS2 + 28		Control	1,633 (0.66)	855 (0.34)	541 (0.43)	551 (0.44)	152 (0.12)			
28	NEUROD1_SNP1			C	G	C/C	C/G	G/G			1.03 (0.91–1.16)
	rs3916026	JPT	Case	893 (0.28)	2,287 (0.72)	132 (0.08)	629 (0.40)	829 (0.52)	0.6685	0.3769	
	−5425		Control	685 (0.28)	1,803 (0.72)	87 (0.07)	511 (0.41)	646 (0.52)			
29	NEUROD1_SNP2			G	T	G/G	G/T	T/T			1.03 (0.90–1.18)
	rs7420169	JPT	Case	2,538 (0.80)	642 (0.20)	1,022 (0.64)	494 (0.31)	74 (0.05)	0.6684	0.6459	
	−5084		Control	1,998 (0.80)	490 (0.20)	803 (0.65)	392 (0.32)	49 (0.04)			
30	ABCC8_SNP1			C	T	C/C	C/T	T/T			1.08 (0.97–1.20)
	rs1799854	JPT	Case	1,507 (0.47)	1,673 (0.53)	371 (0.23)	765 (0.48)	454 (0.29)	0.1664	0.0073†	
	IVS15 −3		Control	1,226 (0.49)	1,262 (0.51)	280 (0.23)	666 (0.54)	298 (0.24)			
31	ABCC8_SNP2			G	A	G/G	G/A	A/A			1.07 (0.91–1.25)
	rs4148643	JPT	Case	2,795 (0.88)	385 (0.12)	1,232 (0.77)	331 (0.21)	27 (0.02)	0.4419	0.7059	
	R1273R		Control	2,169 (0.87)	319 (0.13)	950 (0.76)	269 (0.22)	25 (0.02)			
32	ABCC8_SNP3			T	G	T/T	T/G	G/G			1.07 (0.96–1.19)
	rs757110	JPT	Case	1,884 (0.59)	1,296 (0.41)	570 (0.36)	744 (0.47)	276 (0.17)	0.2432	0.4293	
	S1369A		Control	1,513 (0.61)	975 (0.39)	463 (0.37)	587 (0.47)	194 (0.16)			
33	KCNJ11_SNP1			G	A	G/G	G/A	A/A			1.08 (0.97–1.21)
	rs5219	none	Case	1,954 (0.61)	1,226 (0.39)	610 (0.38)	734 (0.46)	246 (0.15)	0.1513	0.3343	
	E23K		Control	1,576 (0.63)	912 (0.37)	503 (0.40)	570 (0.46)	171 (0.14)			

Locus: experimental name of the SNP, followed by rs number and position. HapMap data: JPT, genotyped on Japanese in Tokyo. Nominal *P* values are listed for allele or genotype frequencies (**P* <0.05; †*P*<0.01). IVS, intron variant sequence.

TABLE 2
Magnitude of LD (D′ and r^2) between *ABCC8* and *KCNJ11* variants

D′/r^2	ABCC8_SNP1	ABCC8_SNP2	ABCC8_SNP3	KCNJ11_SNP1
ABCC8_SNP1 rs1799854	—	0.0012	0.0177	0.0151
ABCC8_SNP2 rs4148643	0.0867	—	0.0919	0.0808
ABCC8_SNP3 rs757110	0.1708	0.9867	—	0.8703
KCNJ11_SNP1 rs5219	0.1653	0.9711	0.9794	—

rs2688, and *NKX2-2*_SNP1 (+856 TGA) and in controls at *NKX6-1*_SNP1 rs1017560 and *ABCC8*_SNP1 rs1799854 (online appendix Table 1). Although none of these are significant with correction for multiple comparisons, we reanalyzed several of the variants, including *NKX2-2*_SNP1 (+856 TGA) and *NKX6-1*_SNP1 rs1017560, and confirmed that there was no typing error for these variants. We also tested whether the observed departures were consistent with the genotype frequencies expected for a genetic disease model (21). The genotype distributions for *TCF2*_SNP5 rs2689, *TCF2*_SNP6 rs2688, *NKX2-2*_SNP1 (+856 TGA), and *ABCC8*_SNP1 rs1799854 are consistent with genetic models that best fit these data. In contrast, the departure from HWE observed in the control samples for *NKX6-1*_SNP1 rs1017560 is not consistent with any genetic model for disease. Thus, the observed departure from HWE in controls at *NKX6-1*_SNP1 rs1017560 is likely to be a chance observation. The remaining departures are unlikely to be attributable to genotyping errors and are consistent with the possibility that the selection of case and control samples from a population in HWE at a susceptibility locus (at the test marker or a polymorphism in strong linkage disequilibrium [LD]) has generated genotype distributions with the observed departures from HWE.

Among the 33 variants of 12 genes, 6 variants (*TCF2*_SNP4 rs1016991, *TCF2*_SNP6 rs2688, *HNF4A*_SNP3 rs745975, *NKX2-2*_SNP2 rs3746741, *NKX6-1*_SNP1 rs1017560, and *ABCC8*_SNP1 rs1799854) showed at least nominally significant associations ($P < 0.05$) with type 2 diabetes (Table 1 and online appendix Table 2). *ABCC8*_SNP1 rs1799854 showed the strongest association ($P = 0.0073$) with diabetes among the SNPs examined in this study. By further analysis of the variant, the T/T genotype was found in 454 (28.6%) and 298 (24.0%) subjects in the diabetic and control groups, respectively, a significant difference in the frequency of individuals with the T/T genotype between the two groups (C/C + C/T vs. T/T, $P = 0.0068$) (online appendix Table 2). The odds ratio (OR) for the T/T genotype was 1.27 (95% CI 1.07–1.50; C/C + C/T vs. T/T), indicating that the T/T genotype in *ABCC8*_SNP1 rs1799854 is associated with type 2 diabetes in Japanese subjects.

There was no association of other variants in *ABCC8* and *KCNJ11* with diabetes (Table 1 and online appendix Table 2). These include the E23K variant in *KCNJ11* (*KCNJ11*_SNP1 rs5219: for the K allele, OR 1.08 [95% CI 0.97–1.21], $P = 0.15$). To determine the extent of LD between the four variants in *ABCC8* and *KCNJ11*, we calculated D′ and r^2 (Table 2). There was modest LD between *ABCC8*_SNP2 rs4148643 and *ABCC8*_SNP3 rs757110. Strong LD was found between *ABCC8*_SNP3 rs757110 and *KCNJ11*_SNP1 rs5219. In the latter, we tested two-locus haplotypes having a frequency of >5% for association with diabetes and found no association of any of the haplotypes with diabetes (data not shown).

We examined the genes involved in pancreatic β-cell function (transcription factors and K_{ATP} channel subunits) in relation to type 2 diabetes in a large cohort of Japanese subjects. The study included 2,834 subjects, the largest case-control study so far conducted on these variants in a Japanese population. For disease susceptibility allele frequencies in the range of 0.3–0.5, our sample had >99% power to detect a susceptibility gene with a genotype relative risk in the range of 1.5–1.85 (for any genetic model of inheritance). For allele frequencies in this range, we had >80% power to detect susceptibility genes with genotype relative risk in the range of 1.25–1.55. Power was similarly good for dominant models with lower susceptibility allele frequencies (0.1–0.3) or recessive models with higher susceptibility allele frequencies (0.5–0.9). The sample was reasonably powered (>90%) to detect recessive susceptibility alleles at low frequencies (0.1–0.3) for higher genotype relative risks (2.1–4.0) but was not sufficiently powered to detect very common (>0.7) dominant susceptibility genes (genotype relative risk >100).

*ABCC8*_SNP1 rs1799854 (exon 16 −3c/t variant) was significantly associated with type 2 diabetes, primarily due to increased frequency of T/T homozygotes among patients. Since this variant is located in the 3′ splice site, it might impair normal splicing. Alternatively, the variant could be in strong LD with an unidentified functional variant in the unscreened region harboring the *ABCC8* gene. There have been two case-control association studies (22,23) conducted for the variant in Japanese populations, both of which found no association of this variant with type 2 diabetes. However, because these studies were based on a relatively small number of subjects (167 subjects in 22; 456 subjects in 23), their power to detect associations is limited. In Caucasians, several studies (7,8,11–13,17) have reported association of the variant with type 2 diabetes, although other studies found no association of the variant with type 2 diabetes (14–16). On the other hand, several studies have reported an association of the E23K variant in *KCNJ11* (*KCNJ11*_SNP1 rs5219 in this study) with type 2 diabetes in Caucasians (9,10,16,18). Recent meta-analyses (19,20) of the variant support this association. Although our present study finds no association of the E23K variant with diabetes in Japanese subjects (for the K allele, OR 1.08 [95% CI 0.97–1.21], $P = 0.15$), 95% CI around the OR overlaps in meta-analysis of European populations, suggesting that our results are not inconsistent with the previous studies on the E23K variant in *KCNJ11*.

The International HapMap Project aims to determine the common patterns of DNA sequence variation in the human genome (24). In the initial phase of the project, genetic data are being gathered from four populations with African, Chinese, Japanese, and European ancestry. Twenty of 33 SNPs used in this study were genotyped on Japanese subjects in the HapMap project, providing important information for determining whether the genes of interest are associated with type 2 diabetes in a Japanese cohort. To